Quaternary Science Reviews 108 (2015) 1–22

Contents lists available at ScienceDirect

Quaternary Science Reviews

journal homepage: www.elsevier.com/locate/quascirev

Calendar-dated glacier variations in the western European Alps during the Neoglacial: the Mer de Glace record, Mont Blanc massif

Melaine Le Roy [a, *], Kurt Nicolussi [b], Philip Deline [a], Laurent Astrade [a], Jean-Louis Edouard [c], Cécile Miramont [d], Fabien Arnaud [a]

[a] EDYTEM, Université de Savoie, CNRS, 73376 Le Bourget du Lac, France
[b] Institute of Geography, University of Innsbruck, 6020 Innsbruck, Austria
[c] Centre Camille Julian, Aix-Marseille Université, CNRS, 13094 Aix-en-Provence, France
[d] IMBE, Aix-Marseille Université, CNRS, 13545 Aix-en-Provence, France

ARTICLE INFO

Article history:
Received 20 February 2014
Received in revised form
29 October 2014
Accepted 31 October 2014
Available online

Keywords:
Holocene
Neoglacial
Glacier chronology
Tree-rings
Dendrochronology
Subfossil wood
Pinus cembra
Mont Blanc
Western Alps

ABSTRACT

Holocene glacier records from the western European Alps are still sparse, although a number of sites are well suited to constraining pre- and early- Little Ice Age (LIA) glacier advances. The present study provides the first dendrochronologically-based and calendar-dated Neoglacial glacier chronology for the Mont Blanc massif, French Alps. It is based on the analysis of over 240 glacially buried *Pinus cembra* subfossil logs and wood remains found either embedded-in-till or as detrital material in the Mer de Glace right lateral moraine. Only a few of the samples were found to be 'formally *in situ*' but we show that some logs were 'virtually *in situ*' (not rooted but showing little or no evidence of reworking) and could be used to accurately reconstruct past glacier margin behavior in space and time. Uncertainties regarding the other samples may relate to original growth location and/or to outer wood decay. The resulting dates (followed by a '+') were therefore considered maximum-limiting ages for glacier advances. The main burial events – interpreted as glacier advances – occurred between ca 1655+ and 1544+ BC, between ca 1230+ and 1105+ BC, between ca 1013+ and 962+/937+ BC, at ca 802–777 BC, after 608+ BC, between 312 and 337 AD, between ca 485+ AD and 606+ AD, between 1120 and 1178 AD, between ca 1248 and 1278+/1296 AD, and after 1352+ AD. These advances predate the late LIA maxima known from historical sources. The magnitude of the advances gradually increased to culminate in three near-Neoglacial maxima during the 7th, 12th and 13th centuries AD, followed by a first LIA/Neoglacial maximum in the second half of the 14th century AD. The pattern of Neoglacial events described here is coherent with Central and Eastern Alpine glacier chronologies. This indicates marked synchronicity of late Holocene glacier variability and forcing at a regional scale, although occasional differences could be detected between 'Western' and 'Eastern' records. The Mer de Glace record also confirms the link between the timing of sediment erosion in a high-elevation glaciated Alpine catchment and subsequent deposition in the sub-alpine Lake Bourget.

1. Introduction

Holocene climate variability has been subject to a great deal of attention in recent decades (Mayewski et al., 2004; Wanner et al., 2008, 2011), mostly due to the emergence of evidence that climate warming during the late 20th/early 21st century has been on a scale that is unprecedented for at least the last millennium (Büntgen and Tegel, 2011; Trachsel et al., 2012) and probably beyond (Marcott et al., 2013; Miller et al., 2013). Consequently, climate researchers need accurate data on the amplitude and timing of Holocene climate change in order to assess the range of natural variability, identify the main forcings, and model future climate variations (Masson-Delmotte et al., 2013).

Abbreviations: BWP, Bronze Age Warm Period; EACC, Eastern Alpine Conifer Chronology; ELA, Equilibrium Line Altitude; FMA, First Millennium Advance; GI, Göschenen 1 Period; GII, Göschenen 2 Period; GA, Great Aletsch Glacier; GO, Gorner Glacier; GP, Gepatsch Glacier; HMA, High Medieval Advance; LBo, Lake Bourget; LBr, Lake Bramant; LG, Lower Grindelwald Glacier; LIA, Little Ice Age; MBM, Mont Blanc Massif; MCA, Medieval Climate Anomaly; MdG, Mer de Glace; MDG, Mer de Glace upper moraine sector; MOTT, Mer de Glace lower moraine sector; MRW, Mean Ring Width; MTL, Minimum Tree Lifespan; NAO, North Atlantic Oscillation; PA, Pasterze Glacier; RLM, Mer de Glace right lateral moraine; TSI, Total Solar Irradiance.

* Corresponding author.
E-mail addresses: melaine.le-roy@univ-savoie.fr, melainleroy@gmail.com (M. Le Roy).

http://dx.doi.org/10.1016/j.quascirev.2014.10.033
0277-3791/

High-elevation environments are particularly sensitive to rapid climate changes (e.g. Gottfried et al., 2012). Reconstructions of Holocene climate variability in the European Alps have been produced using a variety of proxies, including paleoecological indicators of treeline variations (Haas et al., 1998; Tinner and Theurillat, 2003; Nicolussi et al., 2005; Blarquez et al., 2010; Berthel et al., 2012), lithological and geochemical properties of lake sediments (Schmidt et al., 2008; Giguet-Covex et al., 2012), chironomid assemblages (Heiri et al., 2003; Millet et al., 2009; Ilyashuk et al., 2011), and stable isotope ratios of speleothem calcite (Vollweiler et al., 2006; Boch and Spötl, 2011). Limitations of such studies can be either: (i) reconstruction uncertainties resulting from proxy calibration, (ii) the relatively weak chronological constraints and (iii) a marked anthropogenic impact during the late Holocene hindering the identification of a climate signal (e.g. Giguet-Covex et al., 2014).

Glaciers are widely accepted to be reliable indicators of climate variations on inter-annual to multi-millennial timescales (Denton and Karlén, 1973; Hoelzle et al., 2003; Beedle et al., 2009; Six and Vincent, 2014). Glacier length changes are an expression of changes in the glacier's mass balance (mainly influenced by summer temperature and winter precipitation, e.g. Oerlemans, 2001) delayed by a time lag (Müller, 1988; Jóhannesson et al., 1989). They have been successfully used to infer local climatic parameters such as the equilibrium line altitude (ELA) (Klok and Oerlemans, 2003; Lüthi, 2014) or global-scale temperature variations (Leclercq and Oerlemans, 2012). Beyond the instrumental period, glacier records rely on historical documentary evidence for the last few centuries and on glacio-geomorphological (i.e. dating of moraine deposits) or glacio-lacustrine investigations, for the Holocene period.

High-resolution glacier chronologies, that is, continuous chronologies with information at a decadal or sub-decadal scale, are needed in order to assess whether past climate events occurred synchronously and decipher the underlying driving mechanisms (Clague et al., 2009; Winkler and Matthews, 2010; Kirkbride and Winkler, 2012). The only way of achieving this goal for periods older than the last few centuries is the dendrochronological dating of *in situ* glacially-sheared logs in glacier forefields (Luckman, 1995; Nicolussi and Patzelt, 2001; Holzhauser et al., 2005; Wiles et al., 2011). A tight constraint on glacier-fed lake and mire sediment deposition can also yields high-resolution chronologies (e.g. Dahl et al., 2003; Matthews and Dresser, 2008; Bakke et al., 2010), although this is an *indirect* reflection of glacier activity. What is more, there are few suitable lacustrine settings in the Alps (Leemann and Niessen, 1994; Guyard et al., 2013; Simonneau et al., 2014).

Since moraines are deposited by a glacier in balance with the climate, glacio-geomorphologically based chronologies contain valuable paleoclimatic informations. However, most end-moraine ridge stratigraphies provide only partial records of glacier advances that actually occurred (Gibbons et al., 1984; Kirkbride and Brazier, 1998; Kirkbride and Winkler, 2012). This is especially true since the LIA cold period (ca 1270–1860 AD[1]) led to some of the most prominent Holocene glacier advances in the Northern Hemisphere (Davis et al., 2009). This problem can be overcome, at least partly, by studying composite lateral moraine stratigraphies in order to obtain a more complete picture of Neoglacial advances (Röthlisberger and Schneebeli, 1979; Osborn, 1986; Holzhauser and Zumbühl, 1996; Osborn et al., 2001, 2012, 2013; Reyes and Clague, 2004; Koch et al., 2007; Jackson et al., 2008). The Neoglacial is defined here as the second part of the Holocene during which alpine glaciers experienced repeated advances close to the Holocene maxima.

The European Alps (Fig. 1a) are among the best-documented regions worldwide concerning Holocene glacier variations (Nicolussi and Patzelt, 2001; Holzhauser et al., 2005; Joerin et al., 2006, 2008; Nicolussi et al., 2006; Nussbaumer et al., 2007; Holzhauser, 2010; Luetscher et al., 2011; Goehring et al., 2011, 2012; Nicolussi and Schlüchter, 2012; Nussbaumer and Zumbühl, 2012; Schimmelpfennig et al., 2012, 2014). Even so, distribution of dated sites is spatially heterogeneous. Unlike the Central and Eastern Alps where glacio-geomorphological studies have been conducted since the 1960s (see Ivy-Ochs et al., 2009 and references therein), there have been to date very few such studies in the French Alps. Nevertheless, this region occupies a key position with respect to the main atmospheric circulations pathways (prevalence of Atlantic influences in the North and Mediterranean influences in the south; Durand et al., 2009; Fig. 1a) and hosts ~15% of the current Alpine glacier area (Paul et al., 2011; Gardent et al., 2014). Furthermore, the Mont Blanc Massif, northern French Alps (MBM; Fig. 1) has seen the emergence of glaciology as a science from the 18th century, as evidenced by several seminal works (de Saussure, 1779, 1786; Forbes, 1843; Tyndall, 1873; Viollet-le-Duc, 1876; Vallot, 1900).

The aim of the present study was to help fill this knowledge gap by using dates obtained from glacially buried subfossil wood material from the moraine of Mer de Glace to establish a reliable chronology for Neoglacial glacier variations in the MBM. We then compared our chronology with the most accurate glacio-geomorphological and lacustrine evidence for Neoglacial glacier advances in the Alps.

2. Study site

Mer de Glace (hereafter MdG; 45°55′N, 06°55′E) is the largest glacier in the French Alps. It is 11.5-km-long along the flowline, covers an area of 30.4 km^2 (without including former tributary Talèfre Glacier) and spans the elevation range from 4205 m to 1531 m a.s.l. (data: 2008; Gardent et al., 2014; Fig. 1b). Strictly speaking, the term MdG refers to the 5-km-long distal part of the glacier. Average ELA was 2880 m a.s.l. for five of the main north-facing MBM glaciers, which include the Leschaux Glacier (Fig. 1b), for the period 1984–2010 (Rabatel et al., 2013). Mean annual temperature and precipitation at the nearby Chamonix-Le Bouchet weather station (1054 m a.s.l.) were 6.5 °C and 1238 mm, respectively, for the period 1961–1990 (Météo France data).

Measurements of MdG frontal variations extend back to 1878 AD. This record indicates an overall retreat of 1.27 km from 1878 until 2013, and three periods of readvance culminating in 1896 (+174 m), 1931 (+237 m) and 1995 (+143 m) (Reynaud and Vincent, 2000; C. Vincent, pers. comm., 2014). The 'reaction time' of MdG is the longest of all the northward flowing glaciers in the MBM, with the glacier tongue taking 11–25 years to react to a change in summer temperature (Nussbaumer and Zumbühl, 2012). This is 11–15 years longer than the observed frontal lag of the most reactive Bossons Glacier (Martin, 1977; Reynaud, 1993; Le Roy, 2012; Fig. 1b). The MdG 'dendro-reaction time' (*sensu* Pelfini et al., 1997) has been calculated for the 1878–2008 AD period by cross-correlation between the MdG length record and a living *Pinus cembra* chronology distant from 6 km. The best correlation was obtained when setting a 13-years lead of the dendro-record relative

[1] Our definition of the onset of the LIA is based on Alpine glacier evidence. Glacier advances as far as the 1880 AD–1850 AD ice level had already occurred by the late 13th century AD (Nicolussi and Patzelt, 2001; see Section 6.2.7 thereafter) and the first LIA culmination occurred in the 14th century AD (Holzhauser et al., 2005). This accords with a notable decline in summer temperatures after ca 1270 AD (Büntgen et al., 2011).

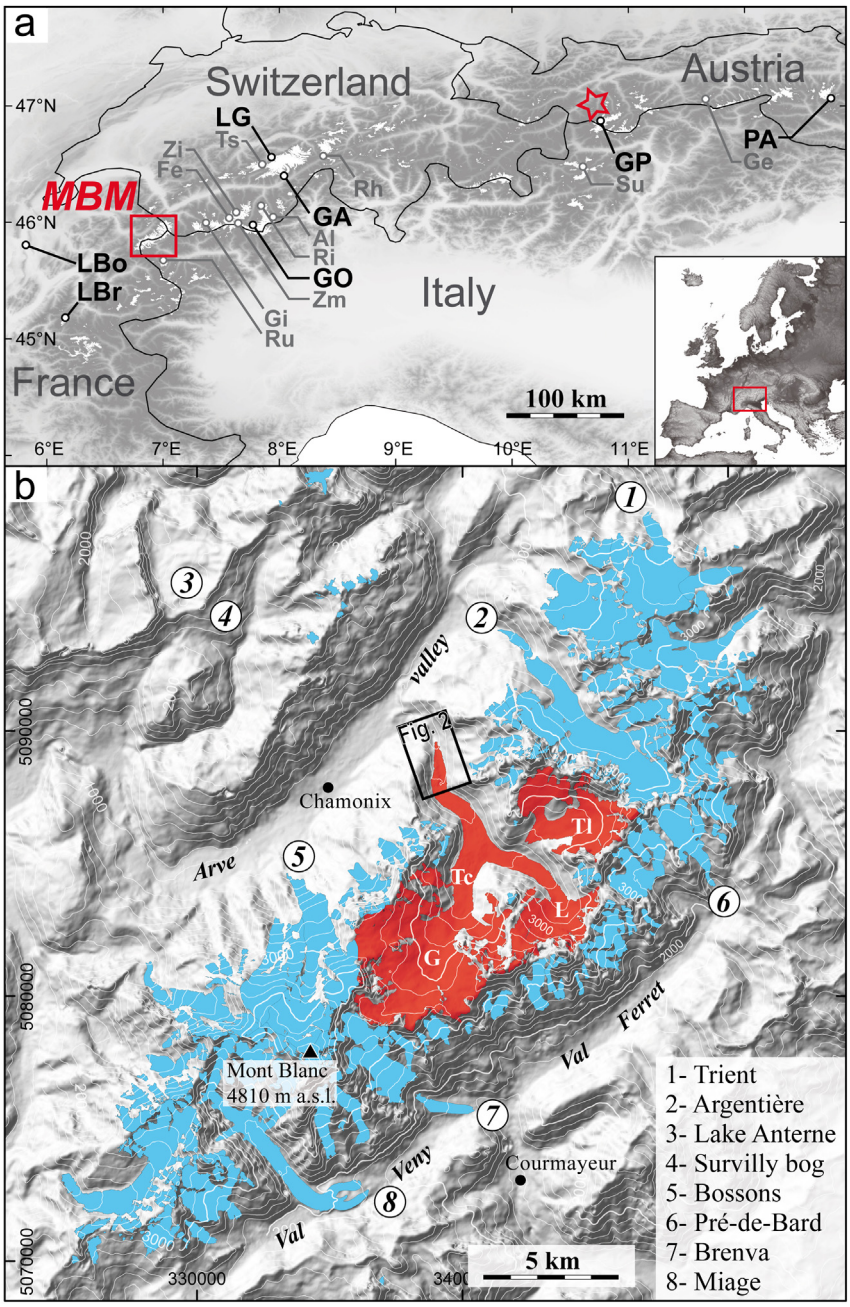

Fig. 1. **(a)** Location of the Mont Blanc Massif (MBM), Lake Bourget (LBo), Lake Bramant (LBr) and locations of high-resolution Neoglacial glacier chronologies available in the Alps, GO: Gorner, LG: Lower Grindelwald, GA: Great Aletsch, GP: Gepatsch, PA: Pasterze. Other Alpine glaciers cited in the text are also indicated, Ru: Rutor, Gi: Giétro, Fe: Ferpècle, Zi: Zinal, Zm: Zmutt, Ri: Ried, Ts: Tschingel, Al: Allalin, Rh: Rhône, Su: Sulden, Ge: Gefrorene Wand. Red star: Main Eastern Alpine Conifer Chronology (EACC) tree megafossils sampling region (Nicolussi et al., 2009). White areas: 2003 glacier extent (Paul et al., 2011). The lower right inset shows the location of the Alps in Europe. **(b)** Shaded-relief map of the MBM showing present-day glacier extent in blue (France, 2008: Gardent et al. (2014); Switzerland, 2010: Fischer et al. (2014); Italy, 2005: RAVA data; Projection UTM 32N). Mer de Glace present and former (late Holocene) tributaries are highlighted in red, G: Géant Glacier, Tc: Tacul Glacier, L: Leschaux Glacier, Tl: Talèfre Glacier. Locations 1 to 8 (all are glaciers except 3 and 4) are mentioned in the text. Approximate location of Fig. 2 is outlined. (For interpretation of the references to color in this figure legend, the reader is referred to the web version of this article.)

to the frontal variations (Le Roy, 2012). The 'volume response time', that is, the minimum time needed by the glacier to adjust to a new climate, is given by the ratio of glacier maximum thickness to ablation at the terminus (Jóhannesson et al., 1989). Using present-day values gave a volume response time of ~38 years. Klok and Oerlemans (2003) used a close formula to calculate an 'analytical length response time', obtaining a value of 56 years for MdG. These data indicate that MdG is able to respond to decadal-scale cold events within an advance/retreat secular trend (Reynaud and Vincent, 2000; Nussbaumer et al., 2007).

The MdG catchment is formed of granite of Late Hercynian age (Bussy and von Raumer, 1994; Leloup et al., 2005). Debris-supply to the glacier tongue mainly results from rockfalls in the accumulation area (e.g. Ravanel et al., 2010) and paraglacial reworking of till material from the lateral moraines. Since the end of the LIA (ca 1860 AD), debris cover on the MdG tongue has expanded (Deline, 2005), with 51% of the glacier ablation zone being debris-covered in 2008 (Deline et al., 2012). The maximum ice thickness was 420 ± 10 m in 1961 at the Tacul Glacier (Fig. 1b), downstream from the Géant icefall (bedrock map in Lliboutry and Reynaud,

1981) and is currently ~380 m at this location (Vincent, 2010). The ice thickness then decreases downstream from this point, with current values of ~160 m near Les Echelets and ~90 m below Montenvers (Fig. 2). Thinning of the tongue has greatly accelerated over the last three decades, from a rate of 0.6 m a^{-1} over the 1979–1994 period to a rate >4 m a^{-1} between 2000 and 2008 (Berthier and Vincent, 2012). This resulted in a 70 m lowering of the tongue below Montenvers since 1990. According to recent models, the terminus of MdG will have retreated another 1200 m by 2040 (Vincent et al., 2014).

The outermost frontal moraine ridges are located in the main valley floor (not visible on Fig. 2) and were deposited during the late stages of the LIA (Mougin, 1912; Wetter, 1987; Nussbaumer et al., 2007 and references therein for a comprehensive overview of previous works on MdG). Total glacier retreat from LIA maxima positions reached in 1644 and 1821 AD (Nussbaumer et al., 2007) amounts to 2.57 km.

The MdG's right lateral moraine (RLM) is typical of marginal deposits from large temperate glaciers (Humlum, 1978; Winkler and Hagedorn, 1999; Curry et al., 2006). It is tens of meters high (up to 180 m directly across from the glacier terminus; Fig. 2) and consists of multiple stacked till units over-consolidated by basal accretion during successive advances (see e.g. Lukas et al., 2012). The MdG's most prominent lateral moraine is on the true right side of the valley. In contrast, moraine deposits were already washed out from the gently inclined bedrock slabs that form most of the left side of the valley in this area (Fig. 2). The study area did not include any discrete lateral moraine ridges, indicating that *superposition* (*sensu* Röthlisberger and Schneebeli, 1979) may have prevailed here, or that the most recently deposited ridges have been eroded away.

Most of the subfossil wood remains we studied were sampled from outcrops at two localities. The locality furthest upstream, labeled the MDG sector, lies between 1910 and 1700 m a.s.l., opposite Montenvers (Fig. 2). The second locality, labeled the MOTT sector, lies between 1700 and 1460 m a.s.l., directly opposite the 'Rochers des Mottets' area of roches moutonnées. It corresponds to the part of the RLM and of the forefield located downstream of the present-day glacier terminus (Fig. 2).

The treeline above the study area roughly follows the 2100 m a.s.l. contour. The timberline is composed of monospecific multi-centennial *P. cembra* stands in the cliffs above the MDG sector while *P. cembra* is mixed with *Larix decidua* above the MOTT sector.

3. Methods

3.1. Sampling procedure

Fieldwork extended over five seasons between 2009 and 2013. Sections of the lateral moraine were surveyed from the opposite side of the valley with a telescope (×30–×70 magnification) to locate the wood outcrops, which were mostly sampled in the fall of 2009 and 2010. Access was achieved by rappelling down the proximal face from the moraine crest and by climbing up gullies from the base of the moraine to reach the lowest till outcrops. Most of the tree remains embedded in the till were within wood layers that extended a few meters to a few tens of meters, some of which contained dozens of debris fragments ranging from centimeter-sized pieces to logs several meters long and 80 cm in diameter. Isolated wood fragments occurred more rarely. Some of these woody layers were in contact with stratigraphical discontinuities such as paleosols, debris-rich litter horizons, or fluvioglacial deposits (stratified gravels and sands). Two stumps were unequivocally *in situ*, that is, rooted in till material. Because interpreting ^{14}C dates from paleosols can be problematic, we focused on taking samples for dendrochronological dating. Few twigs were also sampled in litter layers for radiocarbon dating. A detailed description of the sampled moraine wood outcrops is given in the Online Supplementary Data Appendix 1.

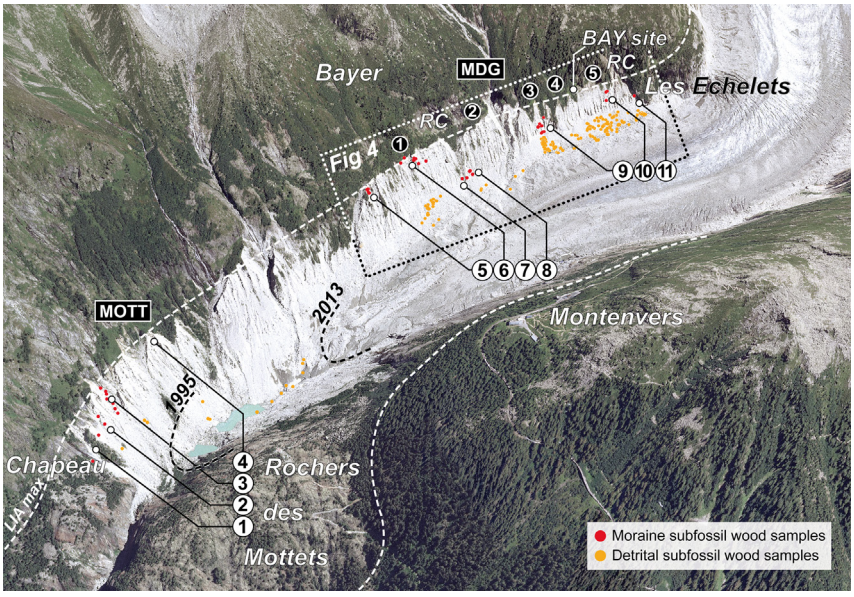

Fig. 2. Oblique aerial view of the MdG forefield based on a 2008 orthophoto (view SE). The two main study areas of the right lateral moraine (RLM) are shown (MDG and MOTT; MDG is divided into 5 sub-sectors). Moraine sample sites are labeled from 1 to 11 (see Appendix 1 for a detailed description of the wood outcrops). Single wood samples are shown by colored dots. RC: Rock cliff areas with *Pinus cembra* stands overlooking the RLM. BAY site: sampling site of dry-dead logs fallen from the above rock cliff which are lying on the surface of the present moraine crest. The MdG LIA maximum extent, as the 1995 and 2013 AD terminus positions are shown with white and black dashed lines, respectively. Horizontal distance between the 1995 AD and 2013 AD frontal positions is 645 m, whereas total retreat between the LIA maxima and the 1995 AD position is 1.92 km. Late-LIA frontal positions in the main valley floor are not visible (bottom left corner). The dotted rectangle shows the position of Fig. 4, and localities cited in the text are indicated. (For interpretation of the references to color in this figure legend, the reader is referred to the web version of this article.)

In addition, we carefully inspected the talus slope below the RLM several times during each field season. We exhaustively sampled all subfossil-appearing tree remains (lying on the surface or partly buried in colluvium) that appeared to have suitably long dendro-series (>ca 60 rings). These repeated surveys allowed us to determine with confidence which of the woody layers in the till some of the reworked samples in the talus had come from (e.g. Appendix 1 Fig. S4c). Moreover, they allowed us to avoid any sampling bias. Because all the sectors were sampled with the same frequency, the age distribution of the samples over time (see Results) accurately reflects the age of the trees actually present in the moraine.

We used a chainsaw to cut least two disks from each log or wood fragment, sampling the best-preserved parts of trunks (e.g. near branches for the eroded logs) to be sure we obtained the longest dendro-series available in each sample. We also sampled bark remains, when present, in order to estimate as accurately as possible the date on which each tree died.

The location of each 'embedded-in-till' moraine sample was measured using a TOPCON total station (accuracy < 1 m), while the location of each talus detrital sample, for which the vertical position was less important, was recorded using a GARMIN handheld GPS (accuracy ± 10 m). The elevation of the moraine crest was recorded above each subfossil wood sampling site. Hence, the position of each sample is given in terms of its vertical distance from the moraine crest.

3.2. Dendrochronological analysis

All the sections were air-dried and sanded with progressively finer paper. We polished the entire surface of each section in order to identify the longest and least disturbed measurement paths. This procedure allowed us to track rings over the whole circumference of a tree trunk, thereby making it easier to identify missing rings. The narrowest rings sectors were prepared with razorblade and chalk powder or water to enhance the definition of rings boundaries. Ring-width measurements were recorded to the nearest 0.01 mm using a LINTAB 5 device associated with the TSAP software package (RinnTech, 2005). We measured at least 3 radii per sample, increasing this number up to 15 in the case of complex paths and/or poorly preserved samples. Radii were then crossdated according to standard dendrochronological procedures and averaged to produce mean individual series. Floating chronologies were built by crossdating the individual series. The synchronization relies on statistical tests including the *Gleichläufigkeit* (Glk) and modified *t*-values (t_{BP}, Baillie and Pilcher, 1973) computed in TSAP, in conjunction with on-screen visual inspection of the curves fit. Microscopic examination and anatomical keys (e.g. Schweingruber, 1990) were used to determine which species each sample belonged to.

Most of the moraine subfossil wood samples exhibit a degree of biological and mechanical alteration (Schweingruber, 2007). Rings were counted but not measured in the altered sectors, and then the counts were added to the end of the measured series in order to obtain better estimates for tree death-dates. We were conservative in our counts of peripheral rings in order to avoid overestimating ages. Therefore, our estimates gave minimum tree lifespan (MTL) that generally ended with a *terminus post quem* for tree death, hereafter called 'virtual death-date' and indicated by a '+'. Because sapwood cannot be identified in subfossil *P. cembra* logs, it was difficult to quantify the number of external rings that had been removed by abrasion. Consequently, we give qualitative confidence levels for the dendro-dates, based on sample preservation and the reliability of the counting (see Appendix 2). Notice that the presence of bark or the last ring (the so-called 'waney edge') does not always mean it is possible to determine the date of tree death to within a year, as the outermost rings may not be countable (Fig. 3; Appendix 2). A pith-offset was estimated when the inner part of a sample was missing. The number of missing years was estimated with help of a Regional Growth Curve build from 335 *P. cembra* individual series sampled in the southern French Alps (Briançonnais area, ~120 km south of MBM; J-L. Edouard, unpublished data).

In areas with a high density of subfossil wood remains and large trunks, we attempted to identify the fragments that originate from a *single tree*. This 'allocation' issue often arises in archaeological contexts (Mom et al., 2011; Tegel et al., 2012; Pichler et al., 2013). We used an expert-based decision process relying on field evidence (i.e. samples from the same site), dendrotypological features (i.e. growth level, growth trend, pith and end-series dates) and crossdating statistics. The highest crossdating value for two definitely different MdG subfossil trees, and the highest crossdating value for subfossil samples from MdG and nearby Argentière Glacier (M. Le Roy, unpublished data) coincide (t_{BP} ~ 10.6). Consequently, we used this threshold as a lower limit for the groupings. Taking this into account, we averaged only highly correlated measures as *single tree* series. We are aware that samples from different heights in a single stem, for example, may be characterized by much lower statistical values, so some groupings may not have been identified. However, this does not affect our glacier advance ages, which are based on the youngest date obtained from each stratigraphically defined wood layer (see Section 5.1 thereafter).

3.3. Absolute dating

As a first step, radiocarbon dating was carried out to anchor floating chronologies in time, and to date samples with too short dendro-series to be reliably crossdated. The samples for radiocarbon dating included 5–15 rings and were taken after dendrochronological analysis, so we knew their exact position in the dendro-series (Appendix 2). Measurements were carried out at the French LMC14 facility in Saclay (Cottereau et al., 2007) and at Beta Analytic Inc. (USA). Radiocarbon dates were calibrated using the CALIB 6.0 program (Stuiver et al., 2011) and INTCAL09 (Reimer et al., 2009). Dating results for samples only constrained by ^{14}C dating are reported by (i) the weighted average of the probability distribution function (Telford et al., 2004) to which we added the distance to the outermost counted ring, and (ii) the 2-sigma calibration range in brackets (Appendix 2).

As no multi-millennial absolutely dated dendrochronological reference curve exists for the French Alps (see Edouard et al., 2002 and Edouard and Thomas, 2008 for an overview of data available in this region) our floating chronologies and single tree series were crossdated with the Eastern Alpine Conifer Chronology (EACC; Nicolussi et al., 2009). This chronology is based on living, dry-dead and subfossil wood mostly from *P. cembra* (82%) sampled at the timberline (2000–2400 m a.s.l.) in the western Austrian Alps (350 km east of MBM; Fig. 1a). In the present paper, all dendrodating results are reported according a time scale that includes a 'year 0' at the beginning of the Common Era (Common Era dates are labeled AD). Consequently, the true historical date of an event before this 'year 0' is one year earlier than the dates reported hereafter and in Appendix 2 (dates before Common Era are labeled BC).

3.4. Deriving an altitudinal glacier variations curve on its lateral margin

In order to constrain MdG Neoglacial variations, we compared the elevation of layers containing subfossil wood remains with known elevation values of the surface of MdG during the 20th century AD taken from field surveys (Reynaud and Vincent, 2000).

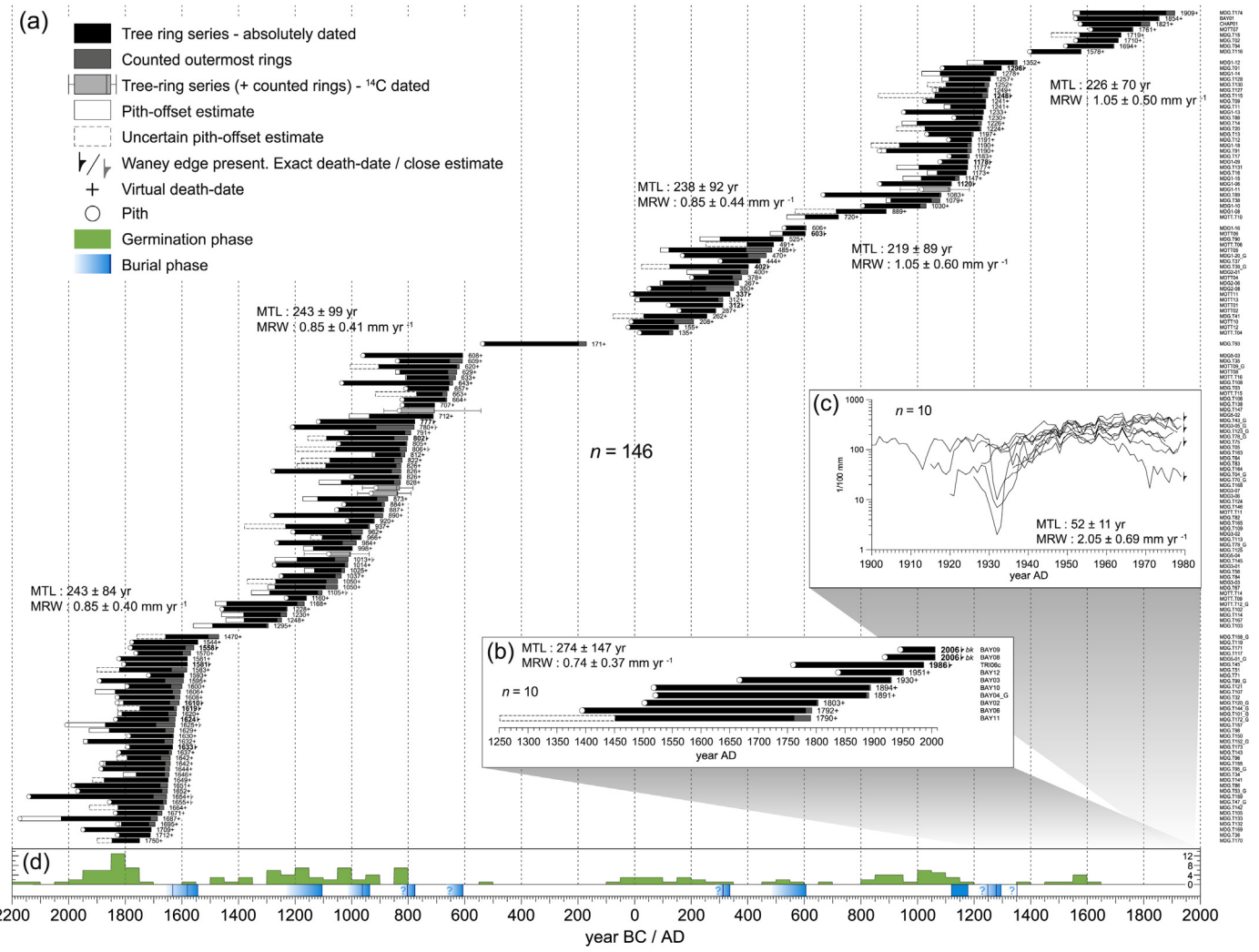

Fig. 3. Ages and lifespans of the trees from the MdG right lateral moraine according to dendrochronological dating. Ages of five samples rely only on radiocarbon dating (thin lines indicate 2-sigma probability interval of calibration). **(a)** Embedded-in-till and detrital subfossil wood remains released from the RLM. Exact tree death-dates (waney edge present, annual counting of outermost rings) are in bold font, close estimates of tree death-dates (waney edge present, conservative counting of outermost rings) and 'virtual' tree death-dates (unknown number of lacking rings) are in regular font. For the close estimates, the waney edge symbol is shown. MTL: minimum tree lifespan (includes pith-offset estimate). MRW: mean ring width for each chronology. **(b)** Dry-dead logs fallen from the rock cliff sampled on the surface of the RLM crest at BAY site (see Fig. 2 and Appendix 1 Fig. S5f). One sample (TRI06c) is from the Trient Glacier moraine crest – similar setting to BAY site (see Fig. 1b for location). Bk: bark present. Note that bark is no longer present after ca 10 years of exposure and waney edge after ca 30 years. **(c)** Crossdating position of modern avalanched trees from Site 7 and nearby colluvium, yielding death-dates in the fall/winter 1979/80 AD. Series are plotted as raw ring-width data. **(d)** Subfossil trees germination and burial phases. Germination phases are depicted as the number of germinating trees during consecutive 50-year intervals. Burial phase timings are based on the most significant samples (i.e. the best-preserved and youngest samples from each wood layer; thin dark blue vertical bars) used to constrain the onset and culmination of the glacier advances (see Section 5.1). (For interpretation of the references to color in this figure legend, the reader is referred to the web version of this article.)

We also drew up profiles across the glacier through the moraine sampling sites from digital elevation models obtained from old maps and photogrammetric surveys. The value retained for comparison with the wood layers elevation was the mean surface elevation of the right-hand margin of the glacier. Twentieth-century analogues for the most extended Neoglacial glacier positions do not exist; therefore, we estimated these positions from the earliest photographs of MdG taken from the mid-19th century AD (Nussbaumer et al., 2007).

4. Results

4.1. Radiocarbon dating

Twenty-eight radiocarbon dates were determined between 310 ± 30 BP and 3390 ± 30 BP (Appendix 2). Additionally, three samples from Site 7 yielded 'modern' ages. Following dendrochronological analyses (see below), ten samples (including five unmeasured twigs) remain only constrained by radiocarbon dating.

4.2. Dendrochronological dating

Dendrochronological measurements were carried out on 240 samples. Absolute dates were obtained for 208 (87%) of these samples. The robustness of the crossdating of MdG *P. cembra* series against the EACC confirms a strong common signal across the Alps (Nicolussi et al., 2009). This high crossdating efficiency was made possible by the fact that 96% of the trees sampled belonged to *P. cembra* L. Other recorded taxa are *Acer* sp., *L. decidua* Mill. and *Picea abies* (L.) Karst (Appendix 2). Among dated series, the 9 samples from the BAY moraine crest site were dry-dead fallen logs from the last millennium, and the 10 modern samples from moraine Site 7

were dated to the late 1970s. All the remaining moraine subfossil samples series were grouped into 141 *single tree* series (as described in Section 3.2).

Fig. 3a presents ages and lifespans of all the subfossil samples that have been dated using dendrochronology and radiocarbon (except the twigs), together with the same data for the dry-dead samples from BAY site (Fig. 3b) and the 20th-century samples from Site 7 (Fig. 3c). The clustering of the subfossil samples allowed the development of five mean ring-width chronologies covering the last four millennia with minor gaps: from 2136 to 1507 BC, 1492 to 608 BC, 23 BC to 522 AD, 523 to 1339 AD and 1396 to 1909 AD. The period from 600 BC to the onset of the Roman Period stands out for the relative lack of subfossil wood remains, as only one sample was recovered. MTL (including pith-offset estimate) ranges from 72+ to 488+ yrs, with a mean of 237 ± 92 yrs, for the subfossil tree samples (except the 20th-century samples). Mean ring-width (MRW) is 0.90 ± 0.49 mm yr^{-1} for the subfossil samples. Fig. 3 shows average MTL and MRW for each chronology. The main phases of tree germination and burial are shown in Fig. 3d in order to provide an overview of stand dynamics, which are partly related to glacier behavior (see Section 5.1) over the last 4 ka (hereafter, ka = calibrated kilo-years BP).

4.3. Geolocation

Spatial data acquired during the field surveys combined with the dates obtained for both the embedded-in-till samples and the detrital samples reveal marked patterns. The results for the MDG sector are shown on Fig. 4. Wood outcrops from each time period are distinct and there is a clear age gradient from upstream to downstream with the oldest samples occurring at the most upstream localities (Sites 10 and 11). The youngest samples are from the Medieval Period (Sites 5 and 6) and occur the furthest downstream. Moreover, Fig. 4 shows that the detrital samples are mostly found just below outcrops of the same age, some of which were sampled, which facilitates assigning detrital samples to known wood layers from the moraine.

5. Interpretation

5.1. Extracting past glacier variability from subfossil logs

Wood found within the glacier forefield must be interpreted with respect to its initial growth location (Röthlisberger et al., 1980; Ryder and Thomson, 1986; Joerin et al., 2008). Field evidence from MdG shows that: (i) few subfossil tree remains can be unambiguously considered *in situ*, i.e. grown at finding place; (ii) trees could have grown on other parts of the RLM than the finding place (i.e. on bedrock outcrops or stabilized moraine ridges) and were killed, transported and deposited during a glacier advance; or (iii) trees could have fallen from surrounding slopes and were deposited either on a former moraine crest, on a former moraine proximal slope, or on the glacier surface prior to burial during a subsequent glacier advance. An overview of the dated sites from the RLM is given in Fig. 5.

(i) The 'modern' BAY01 stump, which is rooted on the present moraine crest at Site 6, and the subfossil MDG5-04 stump from layer 2 at Site 10 (L2/S10; Fig. 5) are examples of unequivocal *in-situ* tree growth on a moraine ridge. Information from such *in situ* samples can be interpreted as being directly related to glacier activity.

(ii) During extensive periods of glacier retreat, it can be assumed that trees grew on bedrock outcrops in the RLM. The high density of subfossil material directly downstream from such sites (e.g. Site 9 and 11; Fig. 4) suggests that the trees were killed by an advance of MdG and then deposited and buried nearby. Therefore, sites on the proximal face of the moraine have recorded glacier advances below the level of the paleomoraine crests. The recolonization of moraine proximal slopes by trees has also been reported at Lower Grindelwald Glacier (Holzhauser and Zumbühl, 1996: 112).

(iii) Finally, stands above the sampling localities could have been a third source of origin for MdG logs. As the slope immediately above the RLM is almost entirely covered with trees and delivers dry-dead wood material to the moraine crest (e.g. at BAY site; Fig. 2) and the glacier surface, it can be assumed

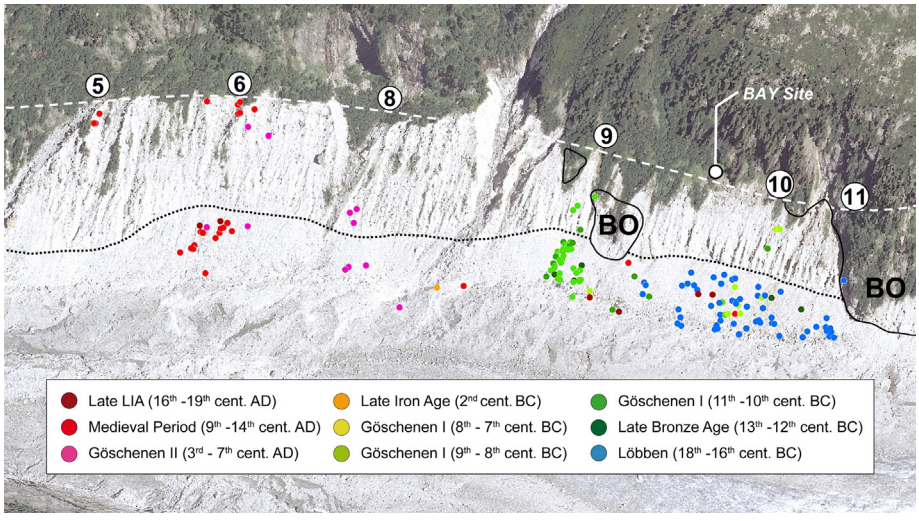

Fig. 4. Spatial distribution of dated subfossil wood samples from the MDG sector (looking ENE, 2008 orthophoto; see Fig. 2 for location). All dated samples are shown, regardless of the groupings that were carried out. Embedded-in-till wood appears under-represented on the figure because it was sampled less exhaustively than detrital wood due to access issues. Moreover, unsampled embedded-in-till wood is not shown here. Consequently, the detrital samples better reflect the actual density of subfossil wood within the RLM. Numbers in circles denote sample sites shown in Fig. 2 (except Site 7 where only 20th-century samples were recovered). The LIA maximum extent and the contact between the till and the talus slope are shown with a white dashed line and a black dotted line, respectively. Bedrock outcrops (BO) located within the RLM are delineated. Length of the exposure is 1.2 km and average height is 100 m. Glacier flow is from right to left.

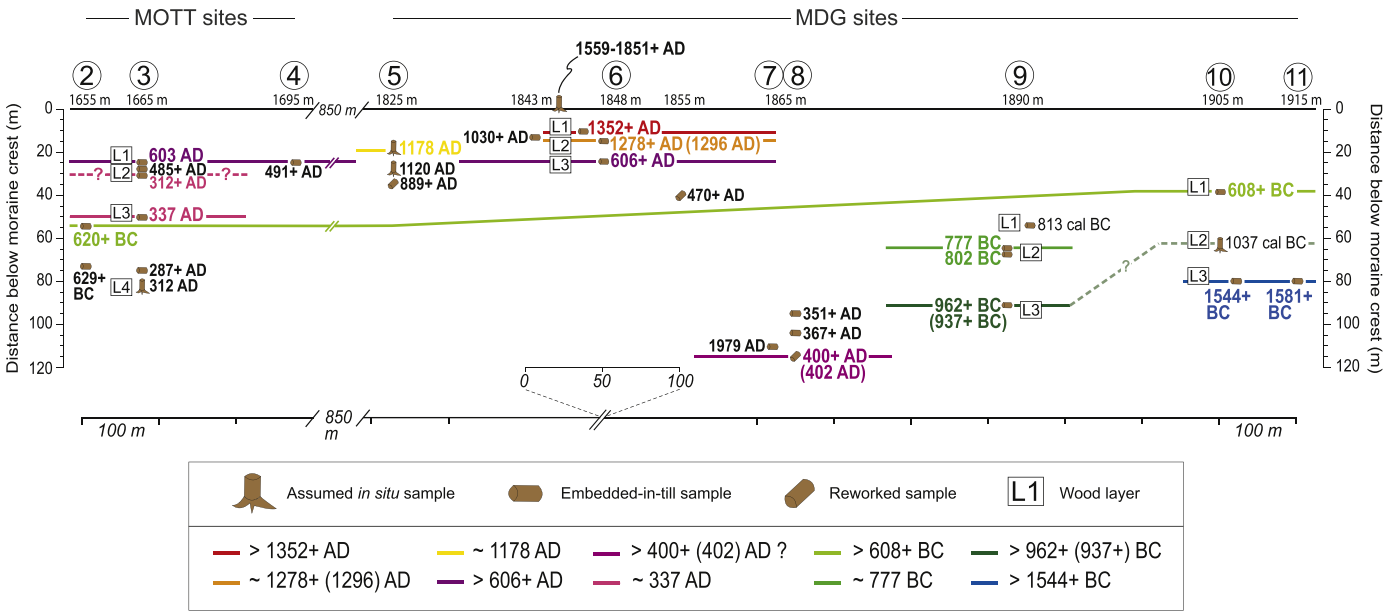

Fig. 5. Summary of dated sites from the MdG right lateral moraine and correlation between layers from the same time periods. Sample locations are given in terms of distance below the moraine crest (upper line with elevation values). Numbers in circles denote sample sites shown in Fig. 2. Colored lines are isochrones showing the position of the glacier margin at the time of burial. The 'assumed *in situ*' symbol includes both the 'formally *in situ*' and 'virtually *in situ*' samples (see Section 5.1). Dates of proposed MdG advances (bottom panel) are based on dating of both embedded-in-till wood remains and – where appropriate – detrital wood remains (in brackets). The Site 1 (LIA reworked samples) is not shown. Glacier flow direction is from right to left. (For interpretation of the references to color in this figure legend, the reader is referred to the web version of this article.)

that analogous processes were also active in the past. Hence, we interpreted large accumulations of eroded woody remains in contact with a paleo-surface (such as L2/S6, Fig. 5; see also Appendix 1 Fig. S3d) as avalanched/dry-dead fallen trees that were subject to differential aerobic decay on a former moraine crest.

Dendrochronological analyses carried out on ten dry-dead logs lying on the present moraine crests at MdG (BAY site) and Trient Glacier (Fig. 1b) suggest that bark and waney edge are preserved for ca 10 years and ca 30 years from tree death, respectively (Fig. 3b). On the other hand, wood remains can be preserved subaerially for up to several centuries in this environment before rotting away (Fig. 3b). These data show that the degree of preservation of the outermost rings indicates the time elapsed between the death of the tree and its burial. Therefore, we interpreted samples that had bark or waney edge over most of their surfaces as having been buried rapidly and only transported a short distance (if any). We refer to these samples as 'virtually *in situ*', as their burial positions record accurate glacier positions at dates that are accurate to within ten years. Conversely, we assumed long exposure or significant reworking when the outermost parts of logs or fragments were shredded, or heavily abraded and incrusted with gravel. In such cases, it is impossible to determine how many outer rings have been removed by erosion.

Although the link between glacier activity and tree death is not always straightforward (particularly in the case of highly weathered fragments), the youngest date in each stratigraphical layer was considered maximum age for the till deposition that buried the layer (Ryder and Thomson, 1986; Reyes and Clague, 2004; Koch et al., 2007). Detrital wood samples from the talus slope at the foot of the RLM are thought to have fallen from contemporaneous wood layers in the same sector (Fig. 4; see also Appendix 1 Fig. S4c). Therefore, in some cases (e.g. detrital samples that were better preserved and/or slightly younger than embedded-in-till samples) these samples were used to complement the information given by the wood samples from the RLM (i.e. a better approximation of the onset and/or the culmination of the advance). Fig. 5 provides maximum-limiting ages for MdG advances, together with correlations between the dated organic levels.

Altitudinal variations of the MdG surface over the last 4 ka determined from the dated moraine sites are shown in Fig. 6. The basic principles followed in order to constrain glacier variations from the subfossil wood record are those used elsewhere (Holzhauser et al., 2005; Holzhauser, 2009, 2010). However, because not all the wood samples were *in situ* and their origin was not always known, our reconstruction had to take into account these uncertainties. When trees are interpreted as 'virtually *in situ*' or when evidence of a paleo-moraine crest were found close to the samples (paleosol, laterally-extensive and debris-rich layer, oxidized horizon), the wood layers are shown in Fig. 6 by the youngest and oldest tree death-dates. These time intervals correspond to periods of tree growth or wood accumulation on former moraine surfaces, without till deposition. Hence, these layers were ice free between these dates, indicating a 'certain' absence of the glacier from this level. Moreover, the oldest germination dates for 'virtually *in situ*' trees or for trees 'of unknown original location' (either from within the glacier forefield or fallen from the slopes) provide evidence for the 'probable' or 'possible' absence of the glacier from the corresponding layer, respectively (Fig. 6).

The magnitude of glacier advances cannot easily be deduced from the vertical spacing of dated wood horizons within lateral moraines (Kirkbride and Winkler, 2012). Nevertheless, we used this spacing to obtain a first order estimate for the Neoglacial advances reconstructed here. The vertical scale used in Fig. 5 is the vertical distance to the moraine crest. However, this scale is not applicable when the relative distance to the crest is not uniform along the entire forefield for a given advance. This is the case when two distant sites marking a medium-sized advance are correlated (e.g. the advance ca 600 BC; see Fig. 5). Consequently Fig. 6 uses known historical elevation values of the MdG surface to provide a homogeneous scale for glacier advances during all periods.

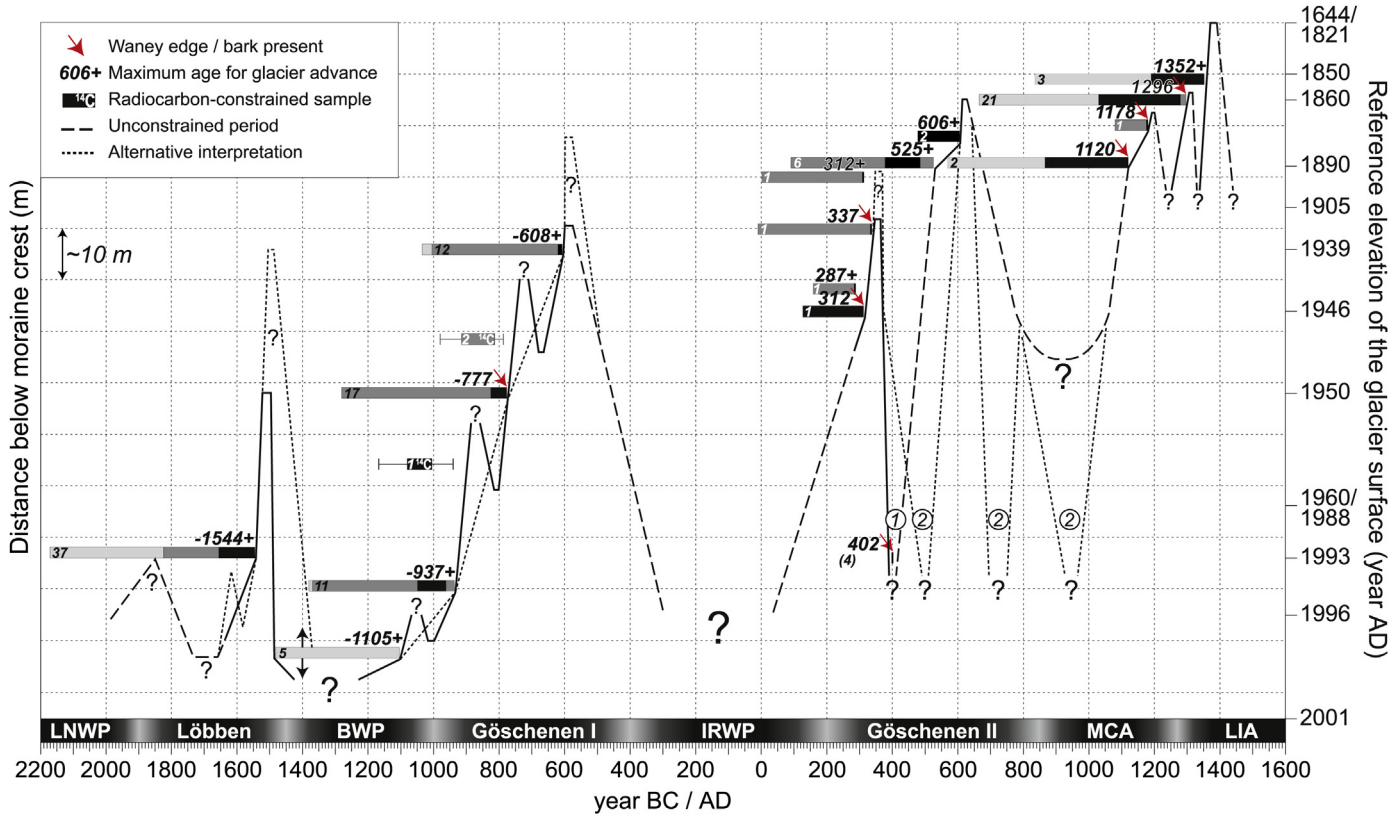

Fig. 6. Altitudinal variations of the MdG surface over the last 4 ka determined from dated subfossil wood layers (horizontal bars) from the right lateral moraine. Glacier variations since 1500 AD are not shown (see Nussbaumer et al., 2007). The rationale behind the construction of the curve can be found in Section 5.1. In order to ensure the different advances throughout the record are represented consistently, the altitudinal position of the wood layers is shown with respect to the mean elevation of the glacier surface opposite the RLM for selected reference years (right-hand scale), rather than by the absolute distance between the wood layers and the moraine crest at each sampling site (left-hand scale, only indicative here). At the elevation of each layer, absence of the glacier is depicted by the length of the bar and ranked as: 'possible' absence (light gray shading), 'probable' absence (medium gray shading), and 'certain' absence (black), based on the interpretation of the wood remains. The number of samples on which the interpretation is based is indicated on the bar. Circled numbers refer to the two possible scenarios arising from the interpretation of the Site 8 samples (see Sections 5.2.5, 6.4.4 and Appendix 1). The altitudinal position of the Bronze Age Warm Period samples is speculative (arrows), as only detrital wood remains were recovered. The samples from L1/S9 (Section 5.2.3) are figured according to the wiggle matching of the two radiocarbon dates (Bronk Ramsey et al., 2001; Appendix 2). LNWP: Late Neolithic Warm Period; BWP: Bronze Age Warm Period; IRWP: Late Iron Age/Roman Age Warm Period; MCA: Medieval Climate Anomaly.

Finally, we must stress that while our record represents glacier thickness variations in front of the subfossil wood layers, related length variations can be assumed as shown by the long time series of direct topographic measurements available at MdG (Reynaud and Vincent, 2000).

5.2. Neoglacial history of MdG inferred from subfossil wood samples

5.2.1. The Löbben Period

The first dated advance of MdG occurred during the Löbben Period (ca 1900–1450 BC – 3.85–3.4 ka; Patzelt and Bortenschlager, 1973). MdG has exceeded the 1993 AD level from 1544+ BC as is shown by the woody layer that occurred at the neighboring Sites 10 and 11. This layer contained the tree MDG.T119_G (sampled on the talus slope but which can be assigned with certainty to L3/S10; Fig. 5) and the only embedded-in-till Löbben-aged log sampled in the RLM, MDG5-01 (1581+ BC; Site 11). Some other well-preserved detrital logs assigned to this layer gave accurate death-dates of between 1593+ and 1558 BC (Appendix 2). These dates may indicate that the advance spanned the first half of the 16th century BC. However, dates of 1655+ and 1654+ BC (not exact death-dates but close estimates) for two waney-edge bearing samples, and clustered exact death-dates obtained from four samples and spanning from 1633 to 1610 BC (Fig. 3a; Appendix 2) suggest that this advance (or an immediately previous one) was already underway as early as the mid-to-late 17th century BC. The preservation of these samples is consistent with a burial episode during the second half of the 17th century BC, most likely around the 1630s–1610s BC.

One sample gave a virtual death-date at 1470+ BC (MDG.T158_G) but we discarded it from our interpretation of the maximum age for the Löbben advance because of the poor preservation of the outer rings of the log, which meant that an unknown and potentially large number of rings was lacking. We cannot completely rule out that it was linked to this advance because it was found close to samples that died during the 16th century BC. However, the most probable explanation for the presence of this tree is that it fell from the slope above onto the proximal face of the moraine deposited during the Löbben advance and was then buried by a rockfall, a mass movement, or a subsequent glacier advance.

The maximum level of the glacier surface during the Löbben advance is not accurately known, although it may have been similar to the 1950 AD level (elevation of L2/S9) or even the 1939 AD level (elevation of L1/S10) (Figs. 5 and 6).

5.2.2. The Bronze Age

Death-dates for five detrital samples are clustered around 1200 BC (1230+ BC to 1105+ BC). We did not include the highly decayed MDG.T103 and MDG.T167 samples in this group, as their estimated dates of death (1295+ and 1248+ BC, respectively;

Appendix 2) could reflect exposure on the surface before the logs were embedded during the late Bronze Age advance.

The retained samples may record a gradual burial episode during an advance whose vertical extent is not known. However, because there is evidence of a probable bedrock outcrop recolonization by trees at L3/S9 from the 14th or 13th century BC, this late Bronze Age advance must have been weaker than the 1993 AD ice level (Fig. 6).

5.2.3. The Göschenen 1 (GI) Period

MdG advanced several times during the GI Period (ca 1000–400 BC – 2.95–2.35 ka; Zoller et al., 1966). A maximum age for the first advance that buried trees is 962+ BC according to dated samples from L3/S9 (Fig. 5) – or 937+ BC if one retains the sufficiently preserved MDG.T109 detrital sample. The close estimate obtained for the death-date of the detrital sample MDG.T145 (1013+ BC) may suggest that this advance was already underway at the turn of the 10th century BC. During this first GI advance, surface of the glacier was approximately at the same level as in 1993 AD (Fig. 6). Dated samples from L2 at the same site show that trees likely grew higher up the bedrock outcrop throughout the 10th century BC, hence this 10th-century BC advance may have reached and exceeded the 1960–1988 AD level, but not the 1950 AD level. The age obtained for the 'formally *in situ*' stump MDG5-04 (L2/S10) at 1037 cal. BC (1131–978 cal. BC) appears slightly 'too old' (Fig. 6). It is not possible to state whether its death was linked to glacier activity, as it may died and remained standing until it was buried during the 10th-century BC advance.

Evidence for a second GI advance is provided by logs from L2/S9, whose death-dates are clustered round the turn of the 8th century BC (802 BC, 780+ BC and 777 BC). This may mean that the rise of the ice margin spanned at least two decades. At this time the glacier has exceeded the 1950 AD level and may have reached the 1939 AD level (elevation of L1/S10). The L1/S9 samples were probably buried during the same advance (Fig. 6), as shown by a virtual death-date based on wiggle-matching of around 813 cal. BC (890–798 cal. BC).

Samples from both Site 2 and 10 indicate that the last advance recorded during the GI Period probably peaked at the end of the 7th century BC (Fig. 5). The best-preserved sample (MDG5-03; L1/S10) was buried shortly after 608+ BC. It is certain that this advance reached the 1939 AD level; however the maximum elevation reached by the glacier surface at that time is unknown. The elevations of L1/S3 and L3/S6 (Fig. 5) suggest that it could have peaked above the 1890 AD level (ca 1870 AD level; Fig. 6). Consequently, the paleo-surface upon which the paleosol in contact with MOTT06 developed (L1/S3; Fig. 5) could have been deposited at that time.

5.2.4. The late Iron Age/early Roman Period

This is the most poorly represented time period in the MdG subfossil wood record (Fig. 3a). Only one detrital sample has been dated from that period (171+ BC) and thus can not be firmly linked to a glacier burial episode.

5.2.5. The Göschenen 2 (GII) Period

Robust evidence for the first advance during the GII Period (ca 200–850 AD – 1.75–1.1 ka; Zoller et al., 1966) is provided by the 'virtually *in situ*' and waney edge-bearing log MOTT01 (−82 m) dated to 312 AD, and the fragments MOTT02 (−75 m) dated to 287+ AD and MOTT11 (−50 m) dated to 337 AD. All these samples record the rising of the ice margin during this event at Site 3 (Fig. 5). Hence, the glacier exceeded the 1946 AD level (MOTT01 location) as early as the beginning of the 4th century AD (Fig. 6). The stratigraphical discontinuity observed near the MOTT11 sampling site (L3/S3) as the presence of organic silt deposits could indicate that the advance peaked at ca 337 AD at a level between the 1939 and 1905 AD glacier extent (Fig. 6). However, dating of MOTT13 (312+ AD), found 30 m below the LIA moraine crest (i.e. 20 m above MOTT11), near layers thought to have been buried during the 6th century AD, does not fit this scheme (Fig. 6). This anomaly may be explained by the fact (i) that some of the outer rings from sample MOTT13 might miss, and (ii) that the first GII advance actually peaked at this level (ca 1890 AD level; question marks in Fig. 5) in the middle of the 4th century AD (see also Section 6.1 thereafter).

Samples from Site 8 show that the first GII advance was followed by a lowering of the glacier surface to below the 1993 AD level at around ca 400+/402 AD. However, this retreat may have occurred later (scenarios ① and ② in Fig. 6; see also the description of Site 8 in Appendix 1 and Section 6.4.4 thereafter).

A renewed progression of MdG may be evidenced by tree death-dates in the late 5th/early 6th century AD at Site 3 (MOTT05, 485+ AD), Site 4 (MOTT.T06, 491+ AD) and Site 6 (MDG1-20_G, 470+ AD, and the detrital log MDG.T90, 525+ AD). However, none of these trees are assumed *in situ*, it is therefore impossible to unambiguously prove that the glacier reached a high-stand at the turn of the 6th century AD (as may evidence the MOTT05 sampling site, L2/S3, at approx. −28 m). Nevertheless, it seems probable that a burial phase occurred at that time. The most reliable evidence for the GII maximum comes from Site 3 (L1) and Site 6 (L3), where two wood fragments (MOTT06 and MDG1-16) both located 24 m below the crest of the moraine (Fig. 5), yielded series that crossdate and give death-dates of 603 and 606+ AD, respectively. MOTT06 was lying in contact with a paleosol that could correspond to the paleo-moraine crest deposited during either the last GI advance (ca 600 BC) or the first GII advance (ca 340 AD). MDG1-16 was in a standing position. However, as the tree has not been entirely excavated, it is impossible to know whether or not it was *in situ*. This GII maximum advance must have reached approximately 15 m below the LIA moraine crest, which is comparable to the level of the glacier surface ca 1860 AD.

5.2.6. The High Medieval Advance (HMA)

Site 5 provides evidence of a HMA (Fig. 5). Two dendro-dated samples record a rise in the level of the ice between 1120 and 1178 AD. Their good preservation and their location near paleo-surfaces greatly minimize growth location uncertainties. This interpretation is reinforced by the five indistinguishable radiocarbon dates obtained across the height of this outcrop (Appendix 1 Fig. S2).

This site is located on the northern edge of MDG sub-sector 1 (Fig. 2), thus, at the end of the Medieval Period the moraine paleo-topography must have been subdued, enabling colonization of its proximal face by trees. Consequently, germination of the 'virtually *in situ*' MDG1-06 tree just prior to 866 AD may record the onset of the medieval glacier retreat and optimal conditions for trees colonization at that site.

The maximum vertical extent reached during this advance exceeded the elevation of MDG1-09 (−19 m; ca 1870 AD level) but could not have reached the level of L2 (−15 m) at the nearby Site 6 (Fig. 5), otherwise the accumulation of logs would have stopped at that time.

5.2.7. The early LIA

Site 6 provided evidence constraining early LIA advances (Fig. 5). Burial of L2 occurred after 1278+ AD, possibly at ca 1296 AD, as indicated by a detrital wood sample with waney edge (MDG.T01) found below the large bedrock outcrop separating MDG sub-sectors 3 and 4 (Fig. 2). The assignment of this sample to L2 is based on its preservation state, which indicates fairly rapid burial. The L1 horizon was buried after 1352+ AD (MDG1-12; Fig. 5). The temporal proximity of the different horizons marking HMA and early LIA

events suggests a period with sustained high glacier levels, interspersed with minor lowerings of the glacier surface (Fig. 6).

The 14th-century AD advance was the largest of the three episodes, and deposited the bulk of the 11 m-thick till upon which the tree BAY01 germinated around 1559 AD (Fig. 5; Appendix 1 Fig. S3b). As the maxima of the 17th and 19th centuries AD (Nussbaumer et al., 2007) did not affect the growth of BAY01, this 14th-century AD advance could have been the most extensive LIA/Neoglacial advance at this site. An alternative scenario can be also proposed. If there has been substantial moraine backwall retreat since the end of the LIA, the late LIA deposits (17th and 19th century AD) may have been slightly higher but may have not been preserved.

5.2.8. The late LIA

The MdG subfossil wood record from this period is sparse. Only a few detrital wood samples (with the exception of the BAY01 *in situ* stump) have been dated between the late 16th and early 19th centuries AD (Fig. 3a). However, it is impossible to determine whether they came from a buried layer that has already been removed by erosion, or if they were dry-dead trees that fell from the cliff, laid some time on the moraine crest, and then fell again due to moraine backwall retreat.

6. Discussion

6.1. Contribution to the Neoglacial glacier history of the Mont Blanc Massif

Our MdG chronology greatly improves the existing MBM Neoglacial chronology which had been based exclusively on ^{14}C dating (Corbel and Le Roy Ladurie, 1963; Vivian, 1975; Bezinge, 1976; Bezinge and Vivian, 1976; Orombelli and Porter, 1982; Aeschlimann, 1983; Bless, 1984; Wetter, 1987; Deline and Orombelli, 2005). The MdG record starts at 3.6 ka and confirms that the Löbben Period led to one of the first Neoglacial high-stands in the Alps, or even to a Neoglacial maxima for some glaciers (Patzelt and Bortenschlager, 1973; Bircher, 1982; Renner, 1982; Patzelt et al., 1990; Wipf, 2001; Nicolussi and Patzelt, 2001; Ivy-Ochs et al., 2009; H. Holzhauser unpublished data, in Holzhauser, 2010: 142, 202; Luetscher et al., 2011; Schimmelpfennig et al., 2012).

The downstream decrease in age of the dated samples from the RLM may be due, at least in part, to the multi-centennial trend for the amplitude of glacier advance to increase during the Neoglacial, from 3.6 ka (Fig. 4). However, this decrease in age may also be the result of differential deposition/erosion of the till mantle. The thinner cover in the upstream sector, in the lee of Les Echelets bedrock outcrop (Fig. 2), may have contributed to exposing older sediments. Hence, the basal part of the RLM was deposited during earlier phases of glacier advance that have not yet been precisely dated in the MBM. So far, only two sites have provided evidence for an older early Neoglacial event, although chronological constraints need to be improved. At Miage Glacier, Deline and Orombelli (2005) argued that damming of the valley by the advancing glacier and the subsequent onset of glacio-lacustrine sedimentation upstream of the dam occurred before ca 4.8 ka. At Argentière Glacier, Bless (1984) dated a wood sample associated with a paleosol 130 m below the moraine crest at 3665 ± 80 BP (2290–1780 cal. BC). This organic layer was stratigraphically distinct from the two closely spaced Löbben layers 30 m higher up the same profile and dated to ca 3300 BP (1860–1220 cal. BC).

Since Wetter (1987)'s survey at MdG, the lowering of the local base level has partly uncovered the lower part of the RLM, which may explain why he did not find any Löbben-aged tree remains. However, some localities sampled by this author probably correspond to some of our sampled sites. Wetter reported dating the GI advance at 2500 ± 75 BP (795–415 cal. BC) for wood samples taken 25–30 m below the moraine crest, which is in line with the stratigraphical level and age obtained for L1/S10 (Fig. 5). On the other hand, a date of 1740 ± 65 BP (130–420 cal. AD) for an *in situ* stump located 30 m below the moraine crest could indicate that the first GII advance actually reached this level at Site 3 (question marks in Fig. 5), as discussed above (Section 5.2.5; see also Appendix 1 Fig. S1).

The HMA (12th century AD) and early LIA advances (13th–14th centuries AD) had probably already been radiocarbon-dated in the MBM. At Trient Glacier, a paleosol 12 m below the moraine crest has been dated to 825 ± 55 BP (1045–1280 cal. AD) and records an advance that reached the 1896 AD level (Bless, 1984) and probably beyond. At Miage Glacier, a trunk fragment embedded-in-till 10 m below the moraine crest has been dated to 900 ± 40 BP (1035–1215 cal. AD) (Deline, 1999). Finally, at MdG, an *in situ* trunk associated with a well-developed paleosol 10 m below the moraine crest has been dated to 730 ± 70 BP (1165–1400 cal. AD) (Wetter, 1987) and could correspond to our L2/S6 (Fig. 5).

The growth location of the *in situ* BAY01 stump at Site 6 (Fig. 5) suggests that the 14th-century AD advance of MdG was probably at least as large as the late LIA advances of the 17th and 19th centuries AD. This assumption is supported elsewhere by a radiocarbon age of 530 ± 40 BP (1310–1445 cal. AD) obtained for a paleosol buried by a till deposit just outboard of the LIA maximum moraine ridge (1818/19 AD) at Pré-de-Bard Glacier (Deline, 2002; Fig. 1b). This indicates that this glacier likely reached its Neoglacial maximum extent during the 14th century AD.

Finally, our study also shed light on the history of vegetation in the area. The presence of *P. cembra* is attested since 8.9 ka in the nearby Fiz massif. Pollen percentages of this taxon were quite high until 4.6 ka, and have since decreased due to deforestation (Survilly Bog, David, 2010; Fig. 1b). Our data suggest the continuous presence of mature stands of *P. cembra* on the Bayer slope above the RLM and in the MdG forefield during the last 4 ka (Fig. 3a). This is striking considering the current scarcity of pure *P. cembra* stands in the MBM and the widespread disappearance of this species in the Western Alps after 5–4 ka (Ali et al., 2005; Finsinger and Tinner, 2007; Blarquez et al., 2010; David, 2010; Berthel et al., 2012). This steep and remote rock slope, which has been little impacted by human activities, may thus have provided a refugium for this species.

6.2. Regional comparison of dendrochronologically-based glacier records

Fig. 7 shows selected records constraining glacier variations during the Neoglacial. In this section we compare the dendrochronologically-based MdG record (Fig. 7a) with available high-resolution glacier records for the Alps: Great Aletsch (GA; Fig. 7b), Gorner (GO), Lower Grindelwald (LG) (Holzhauser and Zumbühl, 1996; Holzhauser, 1997; Holzhauser et al., 2005; Holzhauser, 2009, 2010), Gepatsch (GP; Fig. 7c) and Pasterze (PA) (Nicolussi and Patzelt, 2001; Nicolussi, 2009), as well as with selected data for other Alpine and western North American glaciers.

Basic topographic characteristics and response times for the above mentioned glaciers are given in Table 1 in order to facilitate comparisons. These data indicate that the response times of GA and GO to climate variations are up to twice longer than that of MdG. Similarly, PA has a much longer response time to climate variations than MdG, as shown by its continuous retreat since the end of the LIA (G. Lieb, pers. comm., 2011). In contrast, taking into account the uncertainties related to the Jóhannesson et al. (1989)'s formula, the response times of MdG, GP and LG appear to be quite similar.

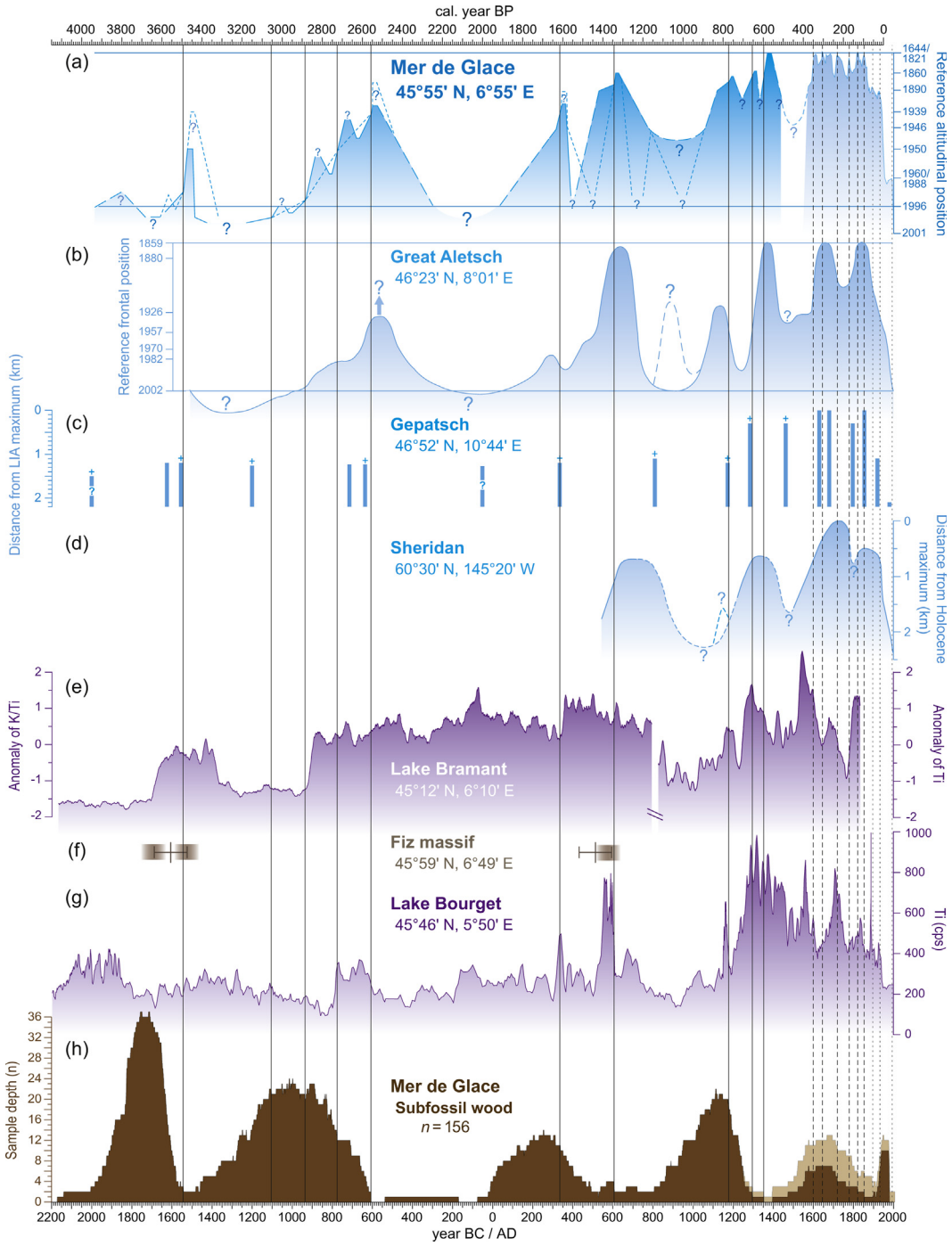

Fig. 7. Comparison of the MdG chronology with regional and global glacier records. **(a)** MdG Neoglacial chronology (this study). The MdG LIA chronology from Nussbaumer et al. (2007) is shown using the same scale (light tones) although it indicates length variations. Vertical solid lines show maximum-limiting ages for the MdG advances derived from the dendro-dated subfossil wood samples. Dashed lines show the late-LIA maxima (bold lines; Nussbaumer et al., 2007) and post-LIA MdG advances (thin lines; Reynaud and Vincent, 2000). **(b)** Great Aletsch Glacier (central Swiss Alps) dendro-based Neoglacial chronology (Holzhauser et al., 2005; Holzhauser, 2009). **(c)** Gepatsch Glacier (western Austrian Alps) dendro-based Neoglacial chronology. The '+' means that the glacier likely exceeded this position to reach an unknown maximum extent (Nicolussi and Patzelt, 2001; Nicolussi, 2009). **(d)** Sheridan Glacier (south-central Alaska) dendro-based late Holocene chronology (Barclay et al., 2013). **(e)** Proglacial Lake Bramant clastic sedimentation (2448 m a.s.l., Grandes Rousses massif; LBr, Fig. 1a). K/Ti anomalies are shown up to 800 AD (left axis); Ti anomalies are shown from 800 AD onwards (right axis). Both anomalies are considered proxies for the Saint-Sorlin Glacier activity during these two time periods (Guyard et al., 2013). **(f)** Detrital events recorded in the Survilly peat bog (2235 m a.s.l., Fiz massif; Fig. 1b) (David, 2010). **(g)** Terrigenous input into sub-alpine Lake Bourget (231 m a.s.l.; LBo, Fig. 1a) recorded by variations in titanium content (Jacob et al., 2008; Arnaud et al., 2012). Data were smoothed using a 3-point running mean. **(h)** Sample depth of the MdG subfossil wood record – includes pith-offset estimates and radiocarbon-dated samples. Light-brown shading shows the adding of the BAY site moraine crest samples. (For interpretation of the references to colour in this figure legend, the reader is referred to the web version of this article.)

Further evidence for this is provided by the correlation between variations in the lengths of MdG and LG over the last 500 years, which gives the best fit with a 1-year lead for MdG (Nussbaumer et al., 2011). However, LG sediment deposition patterns – which do not allow the determination of a magnitude scale for its advances prior to the LIA (H. Holzhauser, pers. comm., 2014) – prevent a full comparison of the two records over the whole Neoglacial period.

Table 1
Basic topographic characteristics and response times of Alpine glaciers for which dendrochronologically-based Neoglacial records are available. Glaciers are listed in descending order of volume response times.

	Length (km)	Surface area (km^2)	Terminus (m a.s.l.)	Mean slope (°)	Max. ice thickness (m)	Reaction time (yr)	Volume response time (yr)	Analytical (numerical) length response time (yr)
Great Aletsch (GA)	23.6	78.4	1649	14.6	800	24	~80	–
Gorner (GO)	13.4	51.5	2173	18.7	450	19	~60	–
Pasterze (PA)	8.3	17.3	2090	15.8	320	–	~40	62 (70–137)
Mer de Glace (MdG)	11.6	30.4	1531	19.3	380	11–25 (13)	~38	56
Gepatsch (GP)	7.5	15.6	2140	12.8	210	–	~26	–
Lower Grindelwald (LG)	8.0	16.7	1376	23.1	230	21	~22	52 (34–45)

Topographic data: Great Aletsch, Gorner and Lower Grindelwald Glaciers: 2011, 2009 and 2011, respectively (Fischer et al., 2014); the area of the Gorner Glacier includes the Grenz Glacier and the recently disconnected Lower Theodul and Breithorn Glaciers; the area of the Lower Grindelwald Glacier includes the recently disconnected Bernese Fiescher and Obers Ischmeer Glaciers; ice thickness data are from Hock et al. (1999), Huss (2005) and Linsbauer et al. (2012), respectively. Mer de Glace: 2008 (Gardent et al., 2014); ice thickness is from Vincent (2010). Pasterze Glacier: 2006 (Lieb and Slupetzky, 2011); mean slope is for 2003 (Paul et al., 2011) and ice thickness is for 1998 (D. Binder, pers. comm., 2014). Gepatsch Glacier: all data are for 2012 (M. Stocker-Waldhuber, pers. comm., 2014).
Response time data: Reaction time values for Aletsch, Gorner and Lower Grindelwald Glaciers are taken from Müller (1988). The Mer de Glace reaction time is taken from Nussbaumer and Zumbühl (2012). The value in brackets is the calculated 'dendro-reaction time' for Mer de Glace (Le Roy, 2012; see Section 2). Volume response time estimates are based on Jóhannesson et al. (1989). Analytical length response times for Pasterze, Mer de Glace and Lower Grindelwald Glaciers are from Klok and Oerlemans (2003). Numerical length response times (in brackets) for Pasterze and Lower Grindelwald Glaciers are from Zuo and Oerlemans (1997) and Schmeits and Oerlemans (1997), respectively. Differences between analytical and numerical values are due to the fact that the numerical models take into account topographical effects (Klok and Oerlemans, 2003).

6.2.1. The Löbben Period

Numerous radiocarbon dates of wood and paleosol have been interpreted as marking multiple advances during the Löbben Period in the Alps (e.g. Bircher, 1982; Renner, 1982; Bless, 1984; Wipf, 2001; see review in Holzhauser, 2010: 140–144) and in the Coast Mountains of British Columbia (Osborn et al., 2013). For example, Wipf (2001) attributed not fewer than four moraine ridges to this period at Tschingel Glacier (Fig. 1a). A first phase of glacier advance may have occurred as early as the 19th century BC as is suggested by a maximum age provided by a detrital wood sample from GO, dendro-dated to 1851+ BC (Holzhauser, 2010). This is in phase with a large germination event identified at MdG around 1825 BC ± 9 yrs ($n = 13, 1\sigma$; Fig. 3d), which may record the recolonization of the forefield by vegetation after a putative first Löbben advance. Then, the maximal MdG subfossil wood sample depth at ca 1760–1700 BC suggests that this first advance was followed by a mild/dry phase (Fig. 7h).

No clear evidence was found at MdG for a multi-phased Löbben Advance Period as is thought to have occurred elsewhere. The obtained accurate death-dates span more than one century (1655–1544 BC) but all the samples (except one) were detrital. Consequently, it is difficult to state whether these trees were buried by a single-phase or a two-phase advance. However, based on (i) what is known about the MdG variations during the LIA (Nussbaumer et al., 2007) and (ii) the fact that accurate death-dates from the mid-to-late 17th century BC (see Section 5.2.1) could indicate a burial event at that time, it appears unlikely that a single advance lasted more than a century. A similar two-step pattern is described at GP where firm evidence show that a first glacier pulse reaching the 1930 AD level occurred between 1660 and 1626 BC, before the slightly larger 16th-century BC advance which exceeded the 1930 AD level (Nicolussi and Patzelt, 2001). Detrital input into the Survilly peat bog also indicates two events constrained by a ^{14}C date of 3557 ± 82 cal. BP (ca 1607 BC) sandwiched between the two detrital layers (David, 2010; Fig. 7f).

At MdG, the Löbben advance peaked after 1544+ BC, but probably no later than 1485–1460 BC as indicated by the germination dates of trees that died during the late Bronze Age advance (Fig. 3a). The virtual death-date of 1470+ BC for detrital sample MDG.T158_G could also represent a minimum age for this advance (see Section 5.2.1). At GP, this advance peaked after 1555 BC, but no later than 1500–1450 BC (Nicolussi and Patzelt, 2001; Fig. 7c). Similarly, at Allalin Glacier (Fig. 1a), the trees that would be killed during the first GI advance germinated after 1458 BC (Röthlisberger et al., 1980; Bircher, 1982; Holzhauser, 2009).

Finally, weakly reactive glaciers experienced significant advance only towards the end of the Löbben Period. For example, peat growth in the PA forefield indicates that the glacier front was upstream of the present terminus between either 1800 and 1550 BC (Nicolussi and Patzelt, 2001) or 1940 and 1430 cal. BC (Kellerer-Pirklbauer and Drescher-Schneider, 2009).

6.2.2. The Bronze Age

At MdG, the Bronze Age Warm Period (BWP) ended with a burial episode that lasted from ca 1230+ BC to 1105+ BC. As it is constrained only by detrital samples, the maximum position reached during this advance is unknown but should lie below the 1993 AD level. At GP, this advance has been recognized at ca 1200 BC (approx. 1940 AD level), albeit also on the basis of a limited amount of detrital samples (Nicolussi and Patzelt, 2001; Nicolussi, 2009). Similar dates have been obtained at GA where the glacier started to advance after the BWP at ca 1213–1211 BC (Holzhauser et al., 2005; Holzhauser, 2009; Fig. 7b).

6.2.3. The Göschenen 1 Period

The GI record is well represented at MdG. Stratigraphical evidence at Sites 9 and 10 shows that at least three discrete advances took place during this period, peaking after 962+/937+ BC, around 777 BC and after 608+ BC. A similar pattern of multiple advances during the GI Period is reported for LG and GP. In contrast, frontal progression of GA appears to have been gradual and almost continuous between ca 1213 BC and 600 BC, punctuated by periods of still-stand (Holzhauser et al., 2005; Holzhauser, 2009). Evidence for a 10th-century BC advance exist also at Allalin Glacier where it is constrained between 959 and 927 BC, when the glacier progression killed 400–500 year-old larch trees (Röthlisberger et al., 1980; Bircher, 1982; Holzhauser, 2009: 195). The maximum extent reached by this reactive glacier was approximately the 1890 AD level. This extent contrasts with GA which did not exceed the 2000 AD level until 941 BC (Holzhauser, 2009).

A very similar picture of the late Bronze Age/early GI Period has been noted in other Northern Hemisphere locations outside the European Alps. For example, a radiocarbon-dated floating ring-width chronology from Geikie Inlet (Glacier Bay, Alaska) indicates that the glacier started to progress into mature forest around 1259–1183 cal. BC (3.21–3.13 ka; see Section 6.2.2 for comparison) and that a major burial event occurred around 974–960 cal. BC (2.92–2.91 ka). The trees killed during this advance germinated between 1650 and 1400 cal. BC (Wiles et al., 2011), which is in line with evidence from the Alps (Section 6.2.1).

Accurate kill-dates of 802, 780+ and 777 BC probably reflect an advance of MdG into a forested moraine proximal face during the second GI advance. At GP, the GI advance had two peaks, dated to shortly after 712 BC and around or after 637 BC. During the 7th century BC it exceeded the 1935 AD level, which is quite similar to MdG, which exceeded at least the 1905 AD level. Broadly speaking, the GI maxima occurred synchronously at MdG, GO and GA, at around 608+, 602 and 600 BC, respectively.

Finally, although high-stands (approx. 1920 AD level) have been reported at Gefrorene Wand Glacier (Eastern Alps; Fig. 1a) around 446+ BC (Nicolussi et al., 2006), we found no evidence for other GI advances after 600 BC at MdG.

6.2.4. The late Iron Age/early Roman Period

This is the period with the weakest dendro-record at MdG. This may be due either to (i) a treeline lowering, which occurred in the Eastern Alps, where it was caused mainly by anthropogenic activity (Nicolussi et al., 2005); such an explanation for the MdG sample gap is unlikely given the continuous presence of trees around MdG throughout the LIA; (ii) a period of sustained high glacier level, which prevented trees recolonizing the forefield; however, this hypothesis is not confirmed by the Lake Bourget (Fig. 1a) record until 150 BC (see Section 6.3 thereafter); or (iii) an extended withdrawal period, which did not allow the burial, and therefore preservation, of the trees. The latter would appear to be the most likely explanation. However, the preservation of the lateral moraine (and therefore of older samples) shows that some glacier advances – that remain to be better characterized – must have occurred during this multi-centennial time period.

6.2.5. The Göschenen 2 Period

The first GII advance was very restricted at GA (approx. the 1982 AD level without exceeding with certainty the 1970 AD level), whereas on more reactive glaciers this advance reached more advanced relative positions: between the 1939 and 1905 AD level – or probably the 1890 AD level – at MdG (Sections 5.2.5 and 6.1), and beyond the 1930 AD level at GP. This advance culminated at very similar dates at GP and MdG: ca 336 and 337 AD, respectively.

Following that advance we propose a retreat centered on 400+/402 AD based on samples from Site 8 (two scenarios for this retreat are discussed in the light of paleoclimatic proxies in Section 6.4.4 thereafter). It should be noted that a possible retreat centered on 370 AD has also been proposed at GA (Holzhauser et al., 2005; H. Holzhauser pers. comm., 2014).

The main discrepancy in the timing of Neoglacial events in the Alps occurred in the second part of the GII Period. The MdG chronology seems to concur with the records for the large Swiss glaciers (GA and GO; Holzhauser et al., 2005; Holzhauser, 2009, 2010), that is, the glaciers had probably already reached advanced positions at the beginning of the 6th century, and advanced to a near-Holocene maximum by the beginning of the 7th century AD. At GA, the timing of this advance is well constrained between 430 AD (1970 AD level) and 590 AD (1870 AD level), with higher progression rates from 532 AD (Holzhauser, 2009), leading to a near-Holocene maximum in the first decades of the 7th century AD. Studies of other Swiss glaciers have given similar dates for this advance (dendro-dates are taken from Holzhauser, 2010; see Fig. 1a for location): Ried Glacier was advancing in ca 525 AD (Holzhauser, 1985: 175), Zmutt Glacier crushed a 400 year-old larch tree in 580 AD (Röthlisberger, 1976: 89), and LG crushed trees between 527 and 595 AD (Holzhauser and Zumbühl, 1996, 2003; Holzhauser, 2009: 190). However, the most advanced positions achieved by these three glaciers at that time are not known precisely (Holzhauser, 2010). This is not the case for Giétro Glacier which reached a size similar to the 1850 AD level in 580 AD (Schneebeli, 1976: 25) and for Rhone Glacier which reached a frontal position ~300 m outboard of the 1856 AD moraine just after 1700 ± 70 BP (140–535 cal. AD) (Zumbühl and Holzhauser, 1988: 229).

On the other hand, evidence from GP, Suldenferner and PA (Eastern Alps; Fig. 1a) indicate that the first millennium AD maximum extent was reached at the beginning of the 9th century (after 809 AD, 834 AD and 1310 ± 70 BP (610–885 cal. AD), respectively), with extents exceeding those of 1920, 1880 and 1925 AD, respectively – and that no maxima occurred at the turn of the 7th century AD (Nicolussi and Patzelt, 2001; Nicolussi et al., 2006; McCormick et al., 2012). Glaciers in the Western Alps have also provided evidence of the early 9th-century AD advance. It is well-constrained for example at LG, where dendro-dates spanning from 823 to 836 AD have been reported (Holzhauser and Zumbühl, 1996, 2003). An advance of Rhône Glacier to a position ~300 m outboard of the 1856 AD moraine just after 1260 ± 65 BP (650–940 cal. AD) can likewise be ascribed to this period (Zumbühl and Holzhauser, 1988: 232). At GO, this advance was more limited, as the glacier exceeded its 1949 AD level but did not exceed its 1940 AD level (Holzhauser, 2010). In the MBM, there is sparse evidence of a prominent 9th-century AD advance, including ^{14}C and dendro-dating of logs at Brenva and Argentière Glaciers (Orombelli and Porter, 1982; Le Roy, 2012).

A working hypothesis that could be drawn from these data is that the '600s AD advance' was the most prominent advance by large glaciers in the Western Alps during the first millennium AD. Although evidence is limited, the '830s AD advance' may have been as important but only for medium-sized glaciers. In contrast, evidence from the Eastern Alps regarding the pre-eminence of the '830s AD advance' are unequivocal. This advance was the largest during the first millennium and there is no evidence for major advances around 600 AD up to now.

The behavior of MdG during the GII Period is also in line with glacier advances described at some western North American sites during the First Millennium Advance (FMA; Reyes et al., 2006). A two-phased FMA advance has been dated at numerous locations in the British Columbia Coast Mountains, with maxima reached around 100–250 cal. AD (1850–1700 cal. BP) and 470–500 cal. AD (1480–1450 cal. BP), separated by a small retreat (Jackson et al., 2008; Hoffman and Smith, 2013). In Alaska, the FMA has been dendro-dated at several glacier forefields, with maxima reached between the 7th and the 10th centuries AD (Barclay et al., 2009, 2013; Wiles et al., 2011; Fig. 7d).

6.2.6. The High Medieval Advance

The MdG record unequivocally shows that a large advance interrupted the Medieval Climate Anomaly (MCA) during the 12th century AD, peaking around 1178 AD (approx. 1870 AD level). In the Alps, other sites where the HMA has been dendro-dated (dendro-dates for Swiss glaciers are taken from Holzhauser, 2010; see Fig. 1a for location) include Ferpècle Glacier (1125 AD; late 19th-century AD level; Röthlisberger et al., 1980: 47), LG (1137 AD; late 19th-century AD level; Holzhauser and Zumbühl, 2003), Zinal Glacier (1159 AD; approx. 1920 AD level; Haas, 1978: 74; Holzhauser, 1985), GP (1172 AD; >1930 AD level; Nicolussi and Patzelt, 2001) and GO (1186 AD; approx. 1949 AD level without exceeding with certainty the 1940 AD level; Holzhauser, 2010). At GA, a maximum age of 1100 AD constrained this advance, corresponding to approximately the 1926 AD level (Holzhauser, 1984: 237–243; Holzhauser et al., 2005). Recent studies have also reported significant glacier advances at that time for a number of western North American glaciers (Koch and Clague, 2011; Barclay et al., 2013).

6.2.7. The early LIA

The two early LIA advances of MdG peaked after 1278+ AD (possibly around 1296 AD) and after 1352+ AD, the latter probably reaching the Holocene maximum.

The 13th-century AD MdG advance is consistent with the onset of the LIA in the Arctic (Miller et al., 2012), southern Alaska (Barclay et al., 2013), the Canadian Rockies (Luckman, 1995; Menounos et al., 2009) and the Alps. In the Western Alps, LG reached a size comparable to its 1850 AD extent in 1246/47 AD (Zumbühl, 1980) and Rutor Glacier is thought to have reached an advanced position (probably similar to the 1880 AD level) in 1284 AD (Aeschlimann, 1983: 76). In the Eastern Alps, some medium-sized glaciers experienced their Holocene maxima at this time (Patzelt, 1995; Patzelt et al., 1996; Zanesco et al., 2008).

The 14th-century AD MdG maximum was synchronous with the first LIA maxima reached by LG (1338 AD), GA (1369 AD) and GO (1385 AD) (Holzhauser et al., 2005). However, the 14th-century AD glacier high-stand seems to have been less extensive in the Eastern Alps. GP exceeded its 1870 AD level in 1284 AD – in line with the first early LIA advance of MdG – and again in 1462 AD, but there is no evidence for a LIA maximum during the 14th century AD (Nicolussi and Patzelt, 2001). Similarly, PA was still smaller than its 1890 AD extent in 1350 AD – as it was from the GII Period to the 17th century AD (Nicolussi and Patzelt, 2001).

6.3. Comparison with regional lake sediment records

We compared our results to the clastic record of the proglacial Lake Bramant (Fig. 7e) located in the Grandes Rousses massif (LBr; Fig. 1a). This record has been interpreted as a proxy for glacier activity in the catchment (Guyard et al., 2013). Moreover, it is particularly sensitive to retreat phases, as the lake catchment only includes the western diffluent part of Saint-Sorlin Glacier (Guyard et al., 2013). Our newly established MdG glacier curve can also be used to test assumptions made about the link between glacier variations in high catchment areas and the rate and origin of sediment deposition in the sub-alpine Lake Bourget[2] (LBo; Fig. 1a; see Arnaud et al., 2005, 2012; Debret et al., 2010). Dendro death-dates providing maximum ages for MdG advances are shown as vertical lines in Fig. 7 together with titanium (Ti) content measured in core LDB04-1 (Fig. 7g). Ti content is a proxy for the terrigenous sediment fraction deposited into LBo by Rhône River flooding events (Debret et al., 2010; Arnaud et al., 2012).

A very significant increase of the K/Ti ratio between 1650 and 1400 cal. BC in the LBr record is highly consistent with our results. This time period encompasses the MdG Löbben advance(s) that began around 1655 BC and peaked after 1544+ BC, indicating that Saint-Sorlin Glacier was also in advanced position at that time. Lake-sediment based reconstructions show a maximum rather centered on 1440 cal. BC (Fig. 7e, g), while there is evidence of tree recolonization of glacier forefields at that time in the Alps (Section 6.2.1). This discrepancy is probably due to the transfer time in sedimentary systems.

The retreat of Saint-Sorlin Glacier during the BWP was followed by a major advance starting around 920 cal. BC (Fig. 7e), which closely corresponds to the first GI advance at MdG, dated to 962+/937+ BC. Advanced positions of Saint-Sorlin Glacier persisted then until 460 cal. BC, which is consistent with high-stands reported for the Austrian Alps at that time (Section 6.2.3). From the GI Period, almost every MdG advance corresponds to a significant detrital peak in LBo. This is particularly clear for the second GI advance dated to 802–777 BC at MdG, which corresponds to a sharp rise in the terrigenous flux peaking around 773 cal. BC in LBo (Fig. 7g). Sustained moderately high levels continue afterward till around 622 cal. BC.

[2] Meltwater from MdG feeds into the Rhône River which flows into LBo during flooding events.

MdG and LBo records then show unambiguous evidence for two distinct events during the GII Period. The first event has been dated to 337 AD at MdG and to ca 342 cal. AD in LBo. The second event is constrained at MdG by two death-dates, 603 and 606+ AD, which are in good agreement with a major Ti peak centered on 586 cal. AD in LBo. In contrast, K/Ti anomalies in LBr sediments show a single peak at that time, between ca 400 and 550 cal. AD.

The HMA is well constrained at MdG by 'virtually *in situ*' and waney edge-bearing wood samples that indicate that the ice margin rose during the 12th century AD, up to a peak around 1178 AD. This agrees well with a short-lived but strong detrital peak around 1163 cal. AD in LBo and a marked Ti anomaly around 1170 cal. AD in LBr. Again, the MdG early-LIA events from the late 13th and mid-14th centuries AD closely corresponds to the lake records. Sedimentological conditions characteristic of the LIA began in both lakes in the late 13th century AD: a first maximum has been reached between 1290 and 1320 cal. AD in LBo whereas the LBr record displays a Ti peak centered on 1295 cal. AD (Fig. 7e, g).

On the other hand, moderate Ti peaks in the LBo record (e.g. 150–100 cal. BC) that do not correspond to known MdG advances, could have an anthropogenic origin. For example, the Lake Anterne flood record suggests that the 400 BC–400 AD time period has been a period of human-induced soil erosion, which blurred the climatic signal (Giguet-Covex et al., 2012, 2014). Nevertheless, further glacier chronology work is needed to clarify this point as there is a body of evidence suggesting an advance during the Roman Period: (i) at MdG, a single tree has been dated to the late Iron Age Period (171+ BC), which is not enough however to highlight a burial episode; (ii) at the nearby Argentière Glacier, a log 15 m below the moraine crest has been dated to 68 cal. BC (197–46 cal. BC; Le Roy, 2012); (iii) at GP, an advance has been proposed around 50 BC (Nicolussi and Patzelt, 2001: 45); and (iv) the LBr record shows a prominent K/Ti anomaly centered on 70 BC, that is of similar magnitude to the anomaly recorded around 500 cal. AD (Guyard et al., 2013; Fig. 7e).

6.4. Climatic control of glacier variations in the Western Alps during the Neoglacial

6.4.1. Solar forcing

The MdG chronology and high-resolution glacier records from the Alps and North America show a high degree of similarity at a multi-decadal scale (Fig. 7a–e), which may indicate a strong common forcing. The sun is the main driver of the Earth's climate system (Gray et al., 2010; Lockwood, 2012). Holocene variations in solar activity have significantly modified the energy balance of the Earth through variations in total solar irradiance (TSI). Many studies have thus claimed that the Holocene climate was paced by solar input (e.g. Bond et al., 2001; Magny, 2004; Magny et al., 2010; van Geel and Mauquoy, 2010) and that this was an important driver of glacier variations (Wiles et al., 2004; Hormes et al., 2006; Koch and Clague, 2006; Nussbaumer et al., 2011). However, the magnitude of TSI changes during the Holocene is controversial as reconstructed values vary greatly (Steinhilber et al., 2009, 2012; Shapiro et al., 2011). In addition, recent modeling efforts have shown that solar forcing probably had only a minor impact on the climate of the Northern Hemisphere during the last millennium (Schurer et al., 2014). Similarly, Lüthi (2014) found no significant relationship between reconstructed ELA series and TSI in the Alps over the last 1600 years, except for the period 1700–1950 AD. Nevertheless, visual comparison of the MdG chronology with a TSI record (Steinhilber et al., 2009) shows that some of the major Neoglacial advances closely correspond to abrupt TSI drop, for example around 1500 BC, 800 BC, 600 AD and 1280 AD (Fig. 8b).

6.4.2. North Atlantic Oscillation (NAO) forcing

In the Alps, the main control of glacier mass balance is summer temperature (e.g. Six and Vincent, 2014). Nevertheless, precipitation (through winter accumulation) has an increasingly large impact on mass balance sensitivity in the western part of the range and close to its northern fringe (e.g. in the MBM), where the climate is moister (Marzeion et al., 2012; Isotta et al., 2014). The most prominent mode of atmospheric variability over Northwestern Europe is the NAO, which is especially pronounced during winter (e.g. Wanner et al., 2001). A positive (negative) NAO mode is characterized by warm/wet (cold/dry) conditions over northern Europe and opposite conditions in southern Europe. However, the impact of the NAO on Alpine climate is ambiguous because the Alps lie in a 'transition zone' between northern and southern Europe, where correlations with the index are generally low or spatially variable (Casty et al., 2005; Lopez Moreno et al., 2011). Despite this,

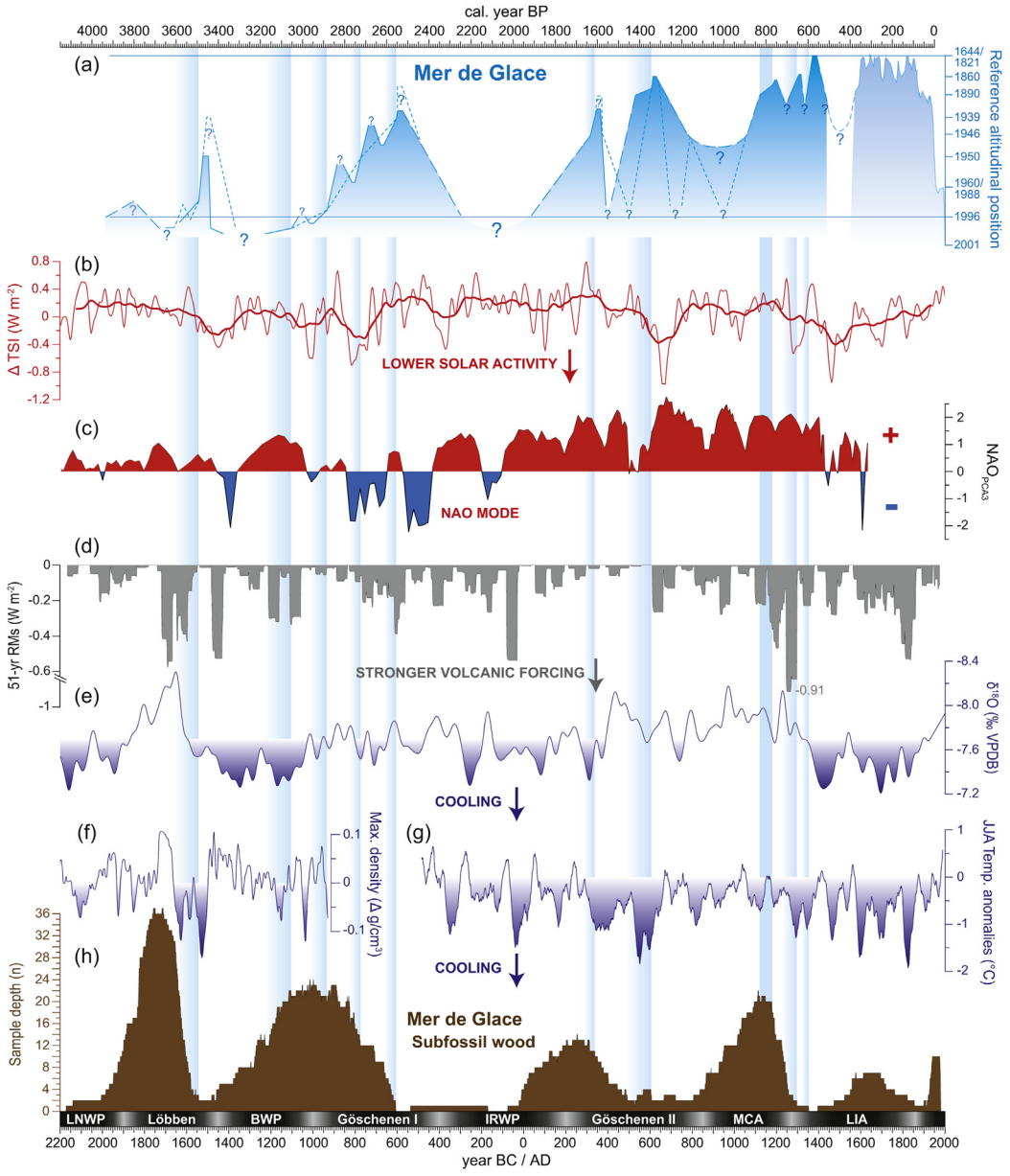

Fig. 8. Comparison of the MdG glacier chronology with main climate forcings and selected Alpine paleoclimate proxies. **(a)** MdG Neoglacial chronology (this study). Vertical blue shadings show periods of tree death (taken from Fig. 3d) interpreted as burial phases by glacier advances. **(b)** Reconstructed total solar irradiance (TSI) from ^{10}Be measured in ice cores (Steinhilber et al., 2009). Bold line is a 31-point running mean smoothing highlighting the multi-centennial trend (original dataset had a 5-year resolution). **(c)** NAO reconstruction based on lake sediments from southwestern Greenland (Olsen et al., 2012). **(d)** Volcanic forcing for the Northern Hemisphere derived from the GISP2 sulfate record. The reconstructed volcanic signals are shown as 51-year running means (Kobashi et al., 2013). The *y*-axis is broken to account for the low values from the 13th century AD. **(e)** COMNISPA δ^{18}O record obtained by stacking data from 3 speleothems from the Spannagel Cave (2310 m a.s.l., Zillertal, western Austria), interpreted as an annual temperature proxy (Vollweiler et al., 2006). **(f)** Maximum latewood density record of subfossil *Larix decidua* logs from the Höhenbiel bog (1960 m a.s.l., Uri, central Switzerland) interpreted as a summer (AS) temperature proxy. The series was smoothed using a 31-year binomial low pass filter (Renner, 1982). **(g)** Reconstructed summer (JJA) temperature anomalies with respect to the 1901–2000 AD period based on EACC material from the Austrian Alps (Büntgen et al., 2011). The record was smoothed using a 31-year running mean. **(h)** Sample depth of the MdG subfossil wood record – includes pith-offset estimates and radiocarbon-dated samples. LNWP: Late Neolithic Warm Period; BWP: Bronze Age Warm Period; IRWP: Late Iron Age/Roman Age Warm Period; MCA: Medieval Climate Anomaly. (For interpretation of the references to color in this figure legend, the reader is referred to the web version of this article.)

several studies in the Western Alps have reported weak to significant anti-correlation on a decadal timescale between the NAO and glacier mass balance (Reichert et al., 2001; Six et al., 2001; Marzeion and Nesje, 2012), glacier length change (Imhof et al., 2012) or glacigenic sedimentation (Guyard et al., 2013). A study at another site from the internal French Alps, 110 km southwest of MBM, did not find any correlation between winter NAO anomalies and the winter mass balance, indicating that precipitation in this area is probably disconnected from the large-scale signal represented by the NAO (Thibert et al., 2013). These studies suggest that the NAO partly controls glacier mass balance in the Northwestern Alps, albeit to a lesser extent than for the more maritime Scandinavian glaciers (Nesje et al., 2000; Reichert et al., 2001; Marzeion and Nesje, 2012). Comparing the MdG chronology with a NAO reconstruction that covers the whole Neoglacial (Olsen et al., 2012) shows that glacier advances seem to be associated with negative or variable NAO phases, at least until the GII Period, and then during the second part of the LIA (Fig. 8c). The persistent positive NAO mode just before and throughout the MCA until the 15th century AD suggests that other forcings were involved in triggering the HMA and early LIA glacier advances.

6.4.3. Volcanic forcing

Volcanic aerosols released during major explosive eruptions reflect and scatter solar radiation, resulting in cooling of the Earth's surface (Robock, 2000; Cole-Dai, 2010). The direct influence of volcanism on temperature appears relatively short-lived (e.g. Esper et al., 2013). However, impact on the climate can be amplified when multiple events occur within a short time period (Sigl et al., 2013; Churakova et al., 2014) and/or by radiative cooling transfer to the ocean (e.g. Stenchikov et al., 2009). Hence, these mechanisms were suggested to be the trigger for the onset of the LIA in the second half of the 13th century AD (Miller et al., 2012) owing to an exceptional cluster of high magnitude eruptive events between 1228 and 1285 AD (Gao et al., 2008). The impact of volcanism on summer precipitation in the year following the eruption has also been reported (Wegmann et al., 2014), likely resulting in highly positive glacier mass balance. Volcanic forcing may thus have been one of the most important decadal-scale drivers of glacier advances during the Neoglacial. Our MdG dendro-record seems to be in line with a significant volcanic forcing. For example, we reconstructed a large advance during the 13th century AD, and this period also stands out by the high frequency of recorded tree death-dates ($n = 12$; Fig. 3a). In addition to the early LIA, volcanic forcing (Gao et al., 2008; Kobashi et al., 2013; Fig. 8d) may likely be identified in the glacier and proxy-derived temperature records during two others periods.

During the Löbben Period, after a mild 'Löbben interstadial' (ca 1760–1660 BC) which is well marked both in paleotemperature proxies and MdG subfossil wood sample depth (Fig. 8e, f, h), the coldest interval lasted from ca 1660 to 1500 BC, with cold peaks centered on ca 1625 BC and ca 1530 BC (Renner, 1982; Fig. 8f). This period is synchronous with a multidecadal-scale strong volcanic event which has been recognized as encompassing the entire 17th century BC (Kobashi et al., 2013; Fig. 8d). Moreover, the first cold peak appear synchronous with the eruption of Thera (Santorini), which has been radiocarbon-dated to between 1660 and 1600 cal. BC (Friedrich et al., 2006), but which could more closely correspond to a growth depression in 1628/27 BC in trees from several Northern Hemisphere locations (Baillie and Munro, 1988; Grudd et al., 2000; Salzer and Hughes, 2007). It is worth noted that the 1650–1550 BC time period is characterized by the highest frequency of tree death-dates in the MdG dendro-record ($n = 25$), surpassing the values for the 13th century AD. However, there is still little direct evidence for a significant impact of volcanism on climate at this time, and the resolution and continuity of the glacier records covering this period are not sufficient (except for GP) to accurately assess the glacier' response to volcanic forcing.

During the GII Period, the so-called '540 AD event' is known to have been an abrupt volcanic-induced cooling that lasted a decade from 536 AD (Baillie, 2008; Larsen et al., 2008; Büntgen et al., 2011; Ferris et al., 2011; Churakova et al., 2014; Fig. 8g). This cooling might have contributed in part to the 6th/early 7th-century AD glacier advance. For example, the highest frontal progression rates of GA during this advance were recorded from the 530s AD (Holzhauser, 2009). However, it seems unlikely that this forcing was solely responsible for the decades of strong ELA lowering reconstructed for this glacier during the 6th century AD (Lüthi, 2014).

Overall, it is probable that the major Neoglacial advances such as those around 600 AD, during the 13–14th centuries AD, and during the second part of the LIA, were caused by the complex interplay of several forcings, including internal variability (Nussbaumer et al., 2011; Wanner et al., 2011).

6.4.4. Comparison with climate proxy records

Our proposed MdG chronology is broadly consistent with independent paleoclimate reconstructions (Fig. 8e–g), which confirm that temperature – mainly from the warm season – was the main driver of MdG fluctuations during the Neoglacial. Only two advances of MdG do not appear to coincide with sharp drops in temperature. These are the last GI advance during the 7th century BC (but summer temperature proxies are lacking for this period) and the HMA during the 12th century AD (Fig. 8). However, a moderate cooling centered on 1120 AD (Fig. 8g) – evidence for which has also been found at a site close to MdG (Millet et al., 2009; Fig. 1b) – could have played a role in triggering the HMA. A further possible driver for this advance is reduced ice ablation due to high cloudiness and low global radiation. The 12th century AD was indeed marked by frequent wet summers in the Alps (Kress et al., 2014).

Another possible discrepancy between available climate reconstructions and the MdG chronology concerns the postulated glacier withdrawal centered on 400 AD. This period was probably cold and wet (Büntgen et al., 2011), therefore unlikely to have driven a marked and rapid glacier retreat as suggested in our scenario ① (Fig. 6). Other candidate periods for such a retreat – allowing the tongue to down-waste to the 1993 AD level – may be found either around 500 AD, around 700 to 750 AD or between 850 and 1050 AD (scenario ② in Fig. 6) according to available paleoclimate evidence (Büntgen et al., 2011; PAGES 2k consortium, 2013). Glacier extents smaller than the present (1985 AD level) have also been inferred for the time period around 550–750 cal. AD from radiocarbon-dated detrital wood samples found in proglacial areas (Joerin et al., 2006).

7. Conclusion

The present research provides the first accurate glacier chronology for the westernmost Alps, establishing a tight temporal constraint for most of the Neoglacial events in this area. The geographical setting of MdG allowed us to obtain a large number of samples which facilitated the recognition of numerous burial episodes. Nevertheless, the scarcity of 'formally *in situ*' trees has somewhat complicated the interpretation of part of the dates we obtained. Dendrochronologically-dated subfossil wood remains from the right lateral moraine have permitted to constrain 10 glacier advances between 1650 BC and 1400 AD. These advances culminated after 1544+ BC (3.49 ka), after 1105+ BC (3.05 ka), after 962+/937+ BC (2.91/2.89 ka), at ca 777 BC (2.73 ka), after 608+ BC (2.56 ka), at ca 337 AD (1.61 ka), after 606+ AD (1.34 ka), at ca 1178 AD (0.77 ka), at ca 1278+/1296 AD (0.67–0.65 ka) and after

1352+ AD (0.60 ka). Most of these advances could be tightly linked to Rhône River flooding events into sub-alpine Lake Bourget, thereby confirming this distal lake-sediment record as a valuable proxy for glacial erosion.

The picture provided by the MdG dendroglaciological record is consistent with other accurate glacier records from the European Alps and western North America. It confirms the generally observed multi-millennial trend of glacier growth culminating during the LIA. Despite a general good agreement at regional scale, the main discrepancies between available 'Western' and 'Eastern' Alpine glacier records come from the first millennium AD (during the GII Period around 500–850 AD – 1.45–1.1 ka) and from the early LIA (14th-century AD advance – 0.6 ka). More work is needed to determine if these discrepancies are due to a lack of preserved evidence, to the response times of the glaciers studied, or if it has a paleoclimatic origin.

Ongoing sampling effort focusing on other glaciers in the MBM (most notably Argentière and Bossons Glaciers) should provide additional data and improve this chronology, particularly regarding several periods that are poorly documented at MdG such as the onset of the Neoglacial around the so-called '4.2 ka event', the Roman Period and the early Medieval Period (9th century AD).

Acknowledgments

MLR's PhD fellowship was funded by the French Ministry of Higher Education and Research (MESR grant 2008-11). KN is supported by the Austrian Science Fund (I 1183-N19). Logistical and analytical support was provided by the French National Research Agency's *Pygmalion* program (ANR BLAN07-2_204489). Most of radiocarbon dating was performed by the national facility LMC14 in the framework of the INSU ARTEMIS call for-proposal. The authors warmly acknowledge Ludovic Ravanel, Emmanuel Malet and Didier Simond for their invaluable help in the field, as Andrea Thurner for tree-ring measurement of some samples. Helpful exchanges with Hanspeter Holzhauser and Andreas Wipf concerning the Neoglacial record of Swiss glaciers were highly appreciated. We are also indebted to Daniel Binder, Mauro Fischer, Samuel Nussbaumer, Martin Stocker-Waldhuber, Christian Vincent and Wolfgang Wetter for sharing personal data. Gerald Osborn and an anonymous reviewer are thanked for the quality of their comments which permitted to greatly improve the manuscript.

Appendix A. Supplementary data

Supplementary data related to this article can be found at http://dx.doi.org/10.1016/j.quascirev.2014.10.033.

References

Aeschlimann, H., 1983. Zur Gletschergeschichte des italienischen Mont Blanc Gebietes: Val Veni – Val Ferret – Ruitor (PhD dissertation). Universität Zürich, 105 pp.

Ali, A.A., Carcaillet, C., Talon, B., Roiron, P., Terral, J.-F., 2005. *Pinus cembra L.* (arolla pine), a common tree in the inner French Alps since the early Holocene and once extended above the present treeline: a synthesis based on charcoal data from soils and travertines. J. Biogeogr. 32, 1659–1669.

Arnaud, F., Revel-Rolland, M., Chapron, E., Desmet, M., Tribovillard, N., 2005. 7200 years of Rhône river flooding activity recorded in Lake Le Bourget: a high resolution sediment record of NW Alps hydrology. Holocene 15, 420–428.

Arnaud, F., Révillon, S., Debret, M., Revel, M., Chapron, E., Jacob, J., Giguet-Covex, C., Poulenard, J., Magny, M., 2012. Lake Bourget regional erosion patterns reconstruction reveals Holocene NW European Alps soil evolution and paleohydrology. Quat. Sci. Rev. 51, 81–92.

Baillie, M.G.L., 2008. Proposed re-dating of the European ice core chronology by seven years prior to the 7th century AD. Geophys. Res. Lett. 35, L15813. http://dx.doi.org/10.1029/2008GL034755.

Baillie, M.G.L., Pilcher, J.R., 1973. A simple cross-dating program for tree-ring research. Tree-ring Bull. 33, 7–14.

Baillie, M.G.L., Munro, M.A.R., 1988. Irish tree rings, Santorini and volcanic dust veils. Nature 332, 344–346.

Bakke, J., Dahl, S.O., Paasche, Ø., Simonsen, J.R., Kvisvik, B., Bakke, K., Nesje, A., 2010. A complete record of Holocene glacier variability at Austre Okstindbreen, northern Norway: an integrated approach. Quat. Sci. Rev. 29, 1246–1262.

Barclay, D.J., Wiles, G.C., Calkin, P.E., 2009. Tree-ring crossdates for a First Millennium AD advance of Tebenkof Glacier, southern Alaska. Quat. Res. 71, 22–26.

Barclay, D.J., Yager, E.M., Graves, J., Kloczko, M., Calkin, P.E., 2013. Late Holocene glacial history of the Copper River Delta, coastal south-central Alaska, and controls on valley glacier fluctuations. Quat. Sci. Rev. 81, 74–89.

Beedle, M.J., Menounos, B., Luckman, B.H., Wheate, R., 2009. Annual push moraines as climate proxy. Geophys. Res. Lett. 36, 20. http://dx.doi.org/10.1029/2009GL039533.

Berthel, N., Schwörer, C., Tinner, W., 2012. Impact of Holocene climate changes on alpine and treeline vegetation at Sanetsch Pass, Bernese Alps, Switzerland. Rev. Palaeobot. Palynol. 174, 91–100.

Berthier, E., Vincent, C., 2012. Relative contribution of surface mass balance and ice flux changes to the accelerated thinning of the Mer de Glace (Alps) over 1979-2008. J. Glaciol. 58 (209), 501–512.

Bezinge, A., 1976. Troncs fossiles morainiques et climat de la période holocène en Europe. Bull. Murithienne 93, 93–111.

Bezinge, A., Vivian, R., 1976. Bilan de la section de glaciologie de la société Hydrotechnique de France: sites sous glaciaires et climat de la période holocène en Europe. La Houille Blanche 6–7, 441–459.

Bircher, W., 1982. Zur Gletscher- und Klimageschichte des Saastales: Glazialmorphologische und dendroklimatologische Untersuchungen. In: Physische Geographie, vol. 9. Zürich, 233 pp.

Blarquez, O., Carcaillet, C., Bremond, L., Mourier, B., Radakovitch, O., 2010. Trees in the subalpine belt since 11 700 cal. BP: origin, expansion and alteration of the modern forest. Holocene 20, 139–146.

Bless, R., 1984. Beträge zur Spät- und Post-glazialen Geschichte der Gletscher im Nordöstlichen Mont Blanc Gebiet. In: Physische Geographie, vol. 15. Zürich, 116 pp.

Boch, R., Spötl, C., 2011. Reconstructing palaeoprecipitation from an active cave flowstone. J. Quat. Sci. 26 (7), 675–687.

Bond, G., Kromer, B., Beer, J., Muscheler, R., Evans, M.N., Showers, W., Hoffmann, S., Lotti-Bond, R., Hajdas, I., Bonani, G., 2001. Persistent solar influence on North Atlantic climate during the Holocene. Science 294, 2130–2136. http://dx.doi.org/10.1126/science.1065680.

Büntgen, U., Tegel, W., 2011. European tree-ring data and the Medieval Climate Anomaly. PAGES 19, 14–15.

Büntgen, U., Tegel, W., Nicolussi, K., McCormick, M., Frank, D., Trouet, V., Kaplan, J., Herzig, F., Heussner, U., Wanner, H., Luterbacher, J., Esper, J., 2011. 2500 years of European climate variability and human susceptibility. Science 331, 578–582.

Bussy, F., von Raumer, J.F., 1994. U-Pb geochronology of Palezoic magmatic events in the Mont Blanc crystalline massif, Western Alps. Schweiz. Mineral. Petrogr. Mittl. 74, 514–515.

Bronk Ramsey, C., van der Plicht, H., Weninger, B., 2001. "Wiggle matching" radiocarbon dates. Radiocarbon 43 (2A), 381–389.

Casty, C., Wanner, H., Luterbacher, J., Esper, J., Böhm, R., 2005. Temperature and precipitation variability in the European Alps since 1500. Int. J. Climatol. 25 (14), 1855–1880.

Churakova (Sidorova), O.V., Bryukhanova, M.V., Saurer, M., Boettger, T., Naurzbaev, M.M., Myglan, V.S., Vaganov, E.A., Hughes, M.K., Siegwolf, R.T.W., 2014. A cluster of stratospheric volcanic eruptions in the AD 530s recorded in Siberian tree rings. Glob. Planet. Change 122, 140–150.

Cole-Dai, J., 2010. Volcanoes and climate. Wiley interdisciplinary reviews. Clim. Change 1, 824–839.

Corbel, J., Le Roy Ladurie, E., 1963. Datation au ^{14}C d'une moraine du Mont Blanc. Rev. Géogr. Alp. 51 (1), 173–175.

Clague, J.J., Menounos, B., Osborn, G., Luckman, B.H., Koch, J., 2009. Nomenclature and resolution in Holocene glacial chronologies. Quat. Sci. Rev. 28, 2231–2238.

Cottereau, E., Arnold, M., Moreau, C., Baqué, D., Bavay, D., Caffy, I., Comby, C., Dumoulin, J.-P., Hain, S., Perron, M., Salomon, J., Setti, V., 2007. Artemis, the new ^{14}C AMS at LMC14 in Saclay, France. Radiocarbon 49, 291–299.

Curry, A.M., Cleasby, V., Zukowskyj, P., 2006. Paraglacial response of steep, sediment-mantled slopes to post- 'Little Ice Age' glacier recession in the central Swiss Alps. J. Quat. Sci. 21 (3), 211–225.

Dahl, S.O., Bakke, J., Lie, Ø., Nesje, A., 2003. Reconstruction of former glacier equilibrium-line altitudes based on proglacial sites: an evaluation of approaches and selection of sites. Quat. Sci. Rev. 22, 275–287.

David, F., 2010. An example of the consequences of human activities on the evolution of subalpine landscapes. C. R. Palevol 9 (5), 229–235.

Davis, P.T., Menounos, B., Osborn, G., 2009. Latest Pleistocene and Holocene alpine glacier fluctuations: a global perspective. Quat. Sci. Rev. 28, 2021–2033.

Debret, M., Chapron, E., Desmet, M., Rolland-Revel, M., Magand, O., Trentesaux, A., Bout-Roumazeille, V., Nomade, J., Arnaud, F., 2010. North western Alps Holocene paleohydrology recorded by flooding activity in Lake Le Bourget. France. Quat. Sci. Rev. 29, 2185–2200.

Deline, P., 1999. Les variations holocènes récentes du glacier du Miage (Val Veny, Val d'Aoste). Quaternaire 10 (1), 5–13.

Deline, P., 2002. Etude géomorphologique des interactions entre écroulements rocheux et glaciers dans la haute montagne alpine: le versant sud-est du massif

du Mont Blanc (Vallée d'Aoste, Italie) (Unpublished PhD thesis). Université de Savoie, 365 pp.
Deline, P., 2005. Change in surface debris cover on Mont Blanc massif glaciers after the 'Little Ice Age' termination. Holocene 15 (2), 302–309.
Deline, P., Orombelli, G., 2005. Glacier fluctuations in the western Alps during the Neoglacial as indicated by the Miage morainic amphiteatre (Mont Blanc massif, Italy). Boreas 34, 456–467.
Deline, P., Gardent, M., Kirkbride, M.P., Le Roy, M., Martin, B., 2012. Geomorphology and dynamics of supraglacial debris covers in the Western Alps. Geophys. Res. Abstr. 14. EGU2012–10866.
Denton, G.H., Karlén, W., 1973. Holocene climatic variations: their pattern and possible cause. Quat. Res. 3, 155–205.
de Saussure, H.-B., 1779. Voyages dans les Alpes, Tome 1. S. Fauche, Neuchâtel, 540 pp.
de Saussure, H.-B., 1786. Voyages dans les Alpes, Tome 2. Barde, Manget et Compagnie, Genève, 641 pp.
Durand, Y., Laternser, M., Giraud, G., Etchevers, P., Lesaffre, B., Mérindol, L., 2009. Reanalysis of 44 yr of climate in the French Alps (1958–2002): methodology, model validation, climatology, and trends for air temperature and precipitation. J. Appl. Meteorol. Climatol. 48 (3), 429–449.
Edouard, J.-L., Guibal, F., Nicault, A., Rathgeber, C., Tessier, L., Thomas, A., Wicha, S., 2002. Arbres subfossiles (*Pinus cembra*, Pinus uncinata et Larix decidua) et évolution des forêts d'altitude dans les Alpes françaises au cours de l'Holocène. Approche dendrochronologique. In: Richard, H., Vignot, A. (Eds.), Actes du colloque international « Equilibre et rupture dans les écosystèmes depuis 20000 ans en Europe de l'Ouest : durabilité et mutation », Annales littéraires, 730, Série "Environnement, Sociétés et Archéologie", Presses Universitaires Francomtoises 3, pp. 403–411.
Edouard, J.-L., Thomas, A., 2008. Cernes d'arbres et chronologie holocène dans les Alpes françaises. In: Desmet, M., Magny, M., Mocci, F. (Eds.), Actes de la Table ronde JurAlp "Dynamique holocène de l'environnement dans le Jura et les Alpes : du climat à l'Homme", Aix en Provence, 15–16 novembre 2007, Collection EDYTEM 6, Chambéry, pp. 179–190.
Esper, J., Schneider, L., Krusic, P.J., Luterbacher, J., Büntgen, U., Timonen, M., Sirocko, F., Zorita, E., 2013. European summer temperature response to annually dated volcanic eruptions over the past nine centuries. Bull. Vocanol. 75, 736. http://dx.doi.org/10.1007/s00445-013-0736-z.
Ferris, D.G., Cole-Dai, J., Reyes, A.R., Budner, D.M., 2011. South Pole ice core record of explosive volcanic eruptions in the first and second millennia A.D. and evidence of a large eruption in the tropics around 535 A.D. J. Geophys. Res. 116, 1–11. http://dx.doi.org/10.1029/2011JD015916.
Finsinger, W., Tinner, W., 2007. Pollen and plant macrofossils at Lac de Fully (2135 m a.s.l.): Holocene forest dynamics on a highland plateau in the Valais, Switzerland. Holocene 17 (8), 1119–1127.
Fischer, M., Huss, M., Hoelzle, M., 2014. The new Swiss Glacier Inventory SGI2010: relevance of using high-resolution source data in areas dominated by very small glaciers. Arct. Antarct. Alp. Res. 46, 4.
Forbes, J.D., 1843. Travels through the Alps of Savoy and Other Parts of the Pennine Chain with Observations of the Phenomena of Glaciers. Adam and Charles Black, Edinburgh, 424 pp.
Friedrich, W.L., Kromer, B., Friedrich, M., Heinemeier, J., Pfeiffer, T., Talamo, S., 2006. Santorini eruption radiocarbon dated to 1627-1600 B.C. Science 312, 548.
Gao, C., Robock, A., Ammann, C., 2008. Volcanic forcing of climate over the past 1500 years: an improved ice core-based index for climate models. J. Geophys. Res. 113 http://dx.doi.org/10.1029/2008JD010239.
Gardent, M., Rabatel, A., Dedieu, J.P., Deline, P., 2014. Multitemporal glacier inventory of the French Alps from the late 1960s to the late 2000s. Glob. Planet. Change 120, 24–37.
Gibbons, A.B., Megeath, J.D., Pierce, K.L., 1984. Probability of moraine survival in a succession of glacial advances. Geology 12, 327–330.
Giguet-Covex, C., Arnaud, F., Enters, D., Poulenard, J., Millet, L., Francus, P., David, F., Rey, P.-J., Wilhelm, B., Delannoy, J.-J., 2012. Frequency and intensity of high altitude floods over the last 3.5 ka in NW European Alps. Quat. Res. 77, 12–22.
Giguet-Covex, C., Pansu, J., Arnaud, F., Rey, P.-J., Griggo, C., Gielly, L., Domaizon, I., Coissac, E., David, F., Choler, P., Poulenard, J., Taberlet, P., 2014. Long livestock farming history and human landscape shaping revealed by lake sediment DNA. Nat. Commun. 5, 3211. http://dx.doi.org/10.1038/ncomms4211.
Goehring, B.M., Schaefer, J.M., Schlüchter, C., Lifton, N.A., Finkel, R.C., Jull, A.J.T., Akçar, N., Alley, R.B., 2011. The Rhone Glacier was smaller than today for most of the Holocene. Geology 39, 679–682.
Goehring, B.M., Vacco, D.A., Alley, R.B., Schaefer, J.M., 2012. Holocene dynamics of the Rhone Glacier, Switzerland, deduced from ice flow models and cosmogenic nuclides. Earth Planet. Sci. Lett. 351-352, 27–35.
Gottfried, M., Pauli, H., Futschik, A., Akhalkatsi, M., Barancok, P., Benito Alonso, J.L., Coldea, G., Dick, J., Erschbamer, B., Fernandez Calzado, M.R., Kazakis, G., Krajci, J., Larsson, P., Mallaun, M., Michelsen, O., Moiseev, D., Moiseev, P., Molau, U., Merzouki, A., Nagy, L., Nakhutsrishvili, G., Pedersen, B., Pelino, G., Puscas, M., Rossi, G., Stanisci, A., Theurillat, J.-P., Tomaselli, M., Villar, L., Vittoz, P., Vogiatzakis, I., Grabherr, G., 2012. Continent-wide response of mountain vegetation to climate change. Nat. Clim. Change 2, 111–115.
Gray, L.J., Beer, J., Geller, M., Haigh, J., Lockwood, M., Matthes, K., Cubasch, U., Fleitmann, D., Harrison, G., Hood, L., Luterbacher, J., Marsh, N., Shindell, D., van Geel, B., White, W., 2010. Solar influences on climate. Rev. Geophys. 48, RG4001. http://dx.doi.org/10.1029/2009RG000282.
Grudd, H., Briffa, K.R., Gunnarsson, B.E., Linderholm, H.W., 2000. Swedish tree rings provide new evidence in support of a major, widespread environmental disruption in 1628 BC. Geophys. Res. Lett. 27, 2957–2960.
Guyard, H., Chapron, E., St-Onge, G., Labrie, J., 2013. Late-Holocene NAO and oceanic forcing on high-altitude alpine proglacial sedimentation (Lake Bramant, Western French Alps). Holocene 23, 1163–1172.
Haas, P., 1978. Untersuchungen zur Gletschergeschichte im Val d'Anniviers (Diploma thesis). University of Zürich, 103 pp.
Haas, J.N., Richoz, I., Tinner, W., Wick, L., 1998. Synchronous Holocene oscillations recorded on the Swiss Plateau and at timberline in the Alps. Holocene 8 (3), 301–309.
Heiri, O., Lotter, A.F., Hausmann, S., Kienast, F., 2003. A chironomid-based Holocene summer air temperature reconstruction from the Swiss Alps. Holocene 13, 477–484.
Hock, R., Iken, A., Wangler, A., 1999. Tracer experiments and borehole observations in the overdeepening of Aletschgletscher, Switzerland. Ann. Glaciol. 28, 253–260.
Hoelzle, M., Haeberli, W., Dischl, M., Peschke, W., 2003. Secular glacier mass balances derived from cumulative glacier length changes. Glob. Planet. Change 36 (4), 77–89.
Hoffman, K.M., Smith, D.J., 2013. Late Holocene glacial activity at Bromley Glacier, Cambria Icefield, northern British Columbia Coast Mountains, Canada. Can. J. Earth Sci. 50, 599–606.
Holzhauser, H., 1984. Zur Geschichte der Aletsch- und des Fiescherngletschers. In: Physische Geographie, vol. 13. Zürich. 448 pp.
Holzhauser, H., 1985. Neue Ergebnisse zur Gletscher- und Klimageschichte des Spätmittelalters und der Neuzeit. Geogr. Helv. 4, 168–185.
Holzhauser, H., 1997. Fluctuations of the Grosser Aletsch Glacier and the Gorner Glacier during the last 3200 years: new results. In: Frenzel, B., Boulton, G.S., Gläser, B., Huckriede, U. (Eds.), Glacier Fluctuations During the Holocene. Paläoklimaforschung, 16, pp. 35–58.
Holzhauser, H., 2009. Auf dem Holzweg zur Gletschergeschichte. In: Hallers Landschaften und Gletscher. Beiträge zu den Veranstaltungen der Akademien der Wissenschaften Schweiz 2008 zum Jubiläumsjahr „Haller 300". Sonderdruck aus den Mitteilungen der Naturforschenden Gesellschaft in Bern. Neue Folge, vol. 66, pp. 173–208.
Holzhauser, H., 2010. Zur geschichte des Gornergletschers – Ein puzzle aus historischen dokumenten und fossilen hölzern aus dem gletschervorfeld. In: Geographica Bernensia, vol. G 84. Institute of Geography, University of Bern, 253 pp.
Holzhauser, H., Zumbühl, H.J., 1996. To the history of the Lower Grindelwald Glacier during the last 2800 years - palaeosols, fossil wood and historical pictorial records - new results. Z. Geomorphol. Neue Folge. Suppl. Bd 104, 95–127.
Holzhauser, H., Zumbühl, H.J., 2003. Jungholozäne Schwankungen des Unteren Grindelwaldgletschers, 54. Deutscher Geographentag Bern. Geographica Bernensia. Geographisches Institut der Universität Bern.
Holzhauser, H., Magny, M., Zumbühl, H.J., 2005. Glacier and lake-level variations in west-central Europe over the last 3500 years. Holocene 15 (6), 789–801.
Hormes, A., Beer, J., Schlüchter, C., 2006. A geochronological approach to understanding the role of solar activity on Holocene glacier length variability in the Swiss Alps. Geogr. Ann. 88A, 281–294.
Humlum, O., 1978. Genesis of layered lateral moraines: implications for paleoclimatology and lichenometry. Geogr. Tidsskr. 77, 65–72.
Huss, M., 2005. Gornergletscher – Gletscherseeausbrüche und Massenbilanzabschätzungen (Unpublished Diploma thesis). VAW-ETH, Zürich.
Ilyashuk, E.A., Koinig, K.A., Heiri, O., Ilyashuk, B.P., Psenner, R., 2011. Holocene temperature variations at a high-altitude site in the Eastern Alps: a chironomid record from Schwarzsee ob Sölden, Austria. Quat. Sci. Rev. 30, 176–191.
Imhof, P., Nesje, A., Nussbaumer, S.U., 2012. Climate and glacier fluctuations at Jostedalsbreen and Folgefonna, southwestern Norway and in the western Alps from the 'Little Ice Age' until the present: the influence of the North Atlantic Oscillation. Holocene 22 (2), 235–247.
Isotta, F.A., Frei, C., Weilguni, V., Perčec Tadić, M., Lassègues, P., Rudolf, B., Pavan, V., Cacciamani, C., Antolini, G., Ratto, S.M., Munari, M., Micheletti, S., Bonati, V., Lussana, C., Ronchi, C., Panettieri, E., Marigon, G., Vertačniko, G., 2014. The climate of daily precipitation in the Alps: development and analysis of a high-resolution grid dataset from pan-Alpine rain-gauge data. Int. J. Climatol. 34, 1657–1675.
Ivy-Ochs, S., Kerschner, H., Maisch, M., Christl, M., Kubik, P.W., Schluchter, C., 2009. Latest Pleistocene and Holocene glacier variations in the European Alps. Quat. Sci. Rev. 28, 2137–2149.
Jackson, S.I., Laxton, S.C., Smith, D.J., 2008. Dendroglaciological evidence for Holocene glacial advances in the Todd Icefield area, northern British Columbia Coast Mountains. Can. J. Earth Sci. 45 (1), 83–98.
Jacob, J., Disnar, J.R., Arnaud, F., Chapron, E., Debret, M., Lallier-Vergès, E., Desmet, M., Revel Rolland, M., 2008. Millet cultivation history in the French Alps as evidenced by a sedimentary molecule. J. Archaeol. Sci. 35, 814–820.
Joerin, U., Stocker, T.F., Schlüchter, C., 2006. Multicentury glacier fluctuations in the Swiss Alps. Holocene 16 (5), 697–704.
Joerin, U., Nicolussi, K., Fischer, A., Stocker, T.F., Schlüchter, C., 2008. Holocene optimum events inferred from subglacial sediments at Tschierva Glacier, Eastern Swiss Alps. Quat. Sci. Rev. 27, 337–350.
Jóhannesson, T., Raymond, C., Waddington, E., 1989. Time-scale for adjustment of glaciers to changes in mass balance. J. Glaciol. 35 (121), 355–369.

Kellerer-Pirklbauer, A., Drescher-Schneider, R., 2009. Glacier fluctuation and vegetation history during the Holocene at the largest glacier of the Eastern Alps (Pasterze Glacier, Austria): new insight based on recent peat findings. In: Proceedings of the 4th Symposium of the Hohe Tauern National Park for Research in Protected Areas, Kaprun, Austria, September 2009, pp. 151–155.
Kirkbride, M.P., Brazier, V., 1998. A critical evaluation of the use of glacial chronologies in climatic reconstruction, with reference to New Zealand. Quat. Proc. 6, 55–64.
Kirkbride, M.P., Winkler, S., 2012. Correlation of Late Quaternary moraines: Impact of climate variability, glacier response, and chronological resolution. Quat. Sci. Rev. 46, 1–29.
Klok, E.J., Oerlemans, J., 2003. Deriving historical equilibrium-line altitudes from a glacier length record by linear inverse modelling. Holocene 13 (3), 343–351.
Kobashi, T., Goto-Azuma, K., Box, J.E., Gao, C.C., Nakaegawa, T., 2013. Causes of Greenland temperature variability over the past 4000 yr: implications for northern hemispheric temperature changes. Clim. Past 9 (5), 2299–2317.
Koch, J., Clague, J.J., 2006. Are insolation and sunspot activity the primary drivers of Holocene glacier fluctuations? PAGES News 14, 20–21.
Koch, J., Clague, J.J., 2011. Extensive glaciers in northwest North America during Medieval time. Clim. Change 107, 593–613.
Koch, J., Osborn, G.D., Clague, J.J., 2007. Pre-'Little Ice Age' glacier fluctuations in Garibaldi Provincial Park, Coast Mountains, British Columbia, Canada. Holocene 17, 1069–1078.
Kress, A., Hangartner, S., Bugmann, H., Büntgen, U., Frank, D.C., Leuenberger, M., Siegwolf, R.T.W., Saurer, M., 2014. Swiss tree-rings reveal warm and wet summers during medieval times. Geophys. Res. Lett. 41, 1732–1737. http://dx.doi.org/10.1002/2013GL059081.
Larsen, L.B., Vinther, M., Briffa, K.R., Melvin, T.M., Clausen, H.B., Jones, P.D., Siggaard-Andersen, M.-L., Hammer, C.U., Eronen, M., Grudd, H., Gunnarson, B.E., Hantemirov, R.M., Naurzbaev, M.M., Nicolussi, K., 2008. New ice core evidence for a volcanic cause of the A.D. 536 dust veil. Geophys. Res. Lett. 35, L04708. http://dx.doi.org/10.1029/2007GL032450.
Leclercq, P.W., Oerlemans, J., 2012. Global and hemispheric temperature reconstruction from glacier length fluctuations. Clim. Dyn. 38, 1065–1079.
Leemann, A., Niessen, F., 1994. Holocene glacial activity and climatic variations in the Swiss Alps: reconstructing a continuous record from proglacial lake sediments. Holocene 4 (3), 259–268.
Leloup, P.H., Arnaud, N., Sobel, E.R., Lacassin, R., 2005. Alpine thermal and structural evolution of the highest external crystalline massif: the Mont Blanc. Tectonics 24, TC4002. http://dx.doi.org/10.1029/2004TC001676.
Le Roy, M., 2012. Reconstitution des fluctuations glaciaires holocènes dans les Alpes occidentales – apports de la dendrochronologie et des datations par isotopes cosmogéniques produits in situ (Unpublished PhD thesis). Université de Savoie, 360 pp.
Lieb, G.K., Slupetzky, H., 2011. Die Pasterze. Der Gletscher am Großglockner. Pustet Verlag, Salzburg, 159 pp.
Linsbauer, A., Paul, F., Haeberli, W., 2012. Modeling glacier thickness distribution and bed topography over entire mountain ranges with GlabTop: application of a fast and robust approach. J. Geophys. Res. 117, F03007. http://dx.doi.org/10.1029/2011JF002313.
Lliboutry, L., Reynaud, L., 1981. 'Global dynamics' of a temperate valley glacier, Mer de Glace, and past velocities deduced from Forbes' bands. J. Glaciol. 27 (96), 207–226.
Lockwood, M., 2012. Solar influence on global and regional climates. Surv. Geophys. ISSN: 1573-0956 33 (3–4), 503–534. http://dx.doi.org/10.1007/s10712-012-9181-3.
López-Moreno, J.I., Vicente-Serrano, S.M., Morán-Tejeda, E., Lorenzo-Lacruz, J., Kenawy, A., Beniston, M., 2011. Effects of the North Atlantic Oscillation (NAO) on combined temperature and precipitation Winter modes in the Mediterranean mountains: observed relationships and projections for the 21st Century. Glob. Planet. Change 77, 62–76.
Luckman, B.H., 1995. Calendar-dated, early 'Little Ice Age' glacier advance at Robson Glacier, British Columbia, Canada. Holocene 5, 149–159.
Luetscher, M., Hoffmann, D.L., Frisia, S., Spötl, C., 2011. Holocene glacier history from alpine speleothems, Milchbach cave, Switzerland. Earth Planet. Sci. Lett. 302, 95–106.
Lukas, S., Graf, A., Coray, S., Schlüchter, C., 2012. Genesis, stability and preservation potential of large lateral moraines of Alpine valley glaciers – towards a unifying theory based on Findelengletscher, Switzerland. Quat. Sci. Rev. 38, 27–48.
Lüthi, M.P., 2014. Little Ice Age climate reconstruction from ensemble reanalysis of Alpine glacier fluctuations. Cryosphere 8, 639–650.
Magny, M., 2004. Holocene climate variability as reflected by mid-European lake-level fluctuations and its probable impact on prehistoric human settlements. Quat. Int. 113, 65–79.
Magny, M., Arnaud, F., Holzhauser, H., Chapron, E., Debret, M., Desmet, M., Leroux, A., Revel, M., Vannière, B., Millet, L., 2010. Solar and proxy-sensitivity imprints on paleohydrological records for the last millennium in westcentral Europe. Quat. Res. 73, 173–179.
Marcott, S.A., Shakun, J.D., Clark, P.U., Mix, A.C., 2013. A reconstruction of regional and global temperature for the past 11,300 years. Science 339, 1198–1201.
Martin, S., 1977. Analyse et reconstitution de la série de bilans annuels du glacier de Sarennes, sa relation avec les fluctuations du niveau de trois glaciers du massif du Mont Blanc (Bossons, Argentière, Mer de Glace). Z. Gletscherkd. Glazialgeol. 13 (1–2), 127–153.
Marzeion, B., Nesje, A., 2012. Spatial patterns of North Atlantic Oscillation influence on mass balance variability of European glaciers. Cryosphere 6, 661–673.
Marzeion, B., Hofer, M., Jarosch, A.H., Kaser, G., Mölg, T., 2012. A minimal model for reconstructing interannual mass balance variability of glaciers in the European Alps. Cryosphere 6, 71–84.
Masson-Delmotte, V., Schulz, M., Abe-Ouchi, A., Beer, J., Ganopolski, A., González Rouco, J.F., Jansen, E., Lambeck, K., Luterbacher, J., Naish, T., Osborn, T., Otto-Bliesner, B., Quinn, T., Ramesh, R., Rojas, M., Shao, X., Timmermann, A., 2013. Information from paleoclimate archives. In: Stocker, T.F., Qin, D., Plattner, G.-K., Tignor, M., Allen, S.K., Boschung, J., Nauels, A., Xia, Y., Bex, V., Midgley, P.M. (Eds.), Climate Change 2013: the Physical Science Basis. Contribution of Working Group I to the Fifth Assessment Report of the Intergovernmental Panel on Climate Change. Cambridge University Press, Cambridge, United Kingdom and New York, NY, USA.
Matthews, J.A., Dresser, P.Q., 2008. Holocene glacier variation chronology of the Smørstabbtindan massif, Jotunheimen, southern Norway, and the recognition of century- to millennial-scale European Neoglacial events. Holocene 18, 181–201.
Mayewski, P.A., Rohling, E.E., Stager, J.C., Karlén, W., Maasch, K.A., Meeker, L.D., Meyerson, E.A., Gasse, F., van Kreveld, S., Holmgren, K., Lee-Thorp, J., Rosqvist, G., Rack, F., Staubwasser, M., Schneider, R.R., Steig, E.J., 2004. Holocene climate variability. Quat. Res. 62, 243–255.
McCormick, M., Büntgen, U., Cane, M.A., Cook, E.R., Harper, K., Huybers, P., Litt, T., Manning, S.W., Mayewski, P.W., More, A.F.M., Nicolussi, K., Tegel, W., 2012. Climate change during and after the Roman Empire: reconstructing the past from scientific and historical evidence. J. Interdiscip. Hist. 43, 169–220.
Menounos, B., Osborn, G., Clague, J.J., Luckman, B.H., 2009. Latest Pleistocene and Holocene glacier fluctuations in western Canada. Quat. Sci. Rev. 28, 2049–2074.
Miller, G.H., Geirsdóttir, A., Zhong, Y., Larsen, D.J., Otto-Bliesner, B.L., Holland, M.M., Bailey, D.A., Refsnider, K.A., Lehman, S.J., Southon, J.R., Anderson, C., Björnsson, H., Thordarson, T., 2012. Abrupt onset of the Little Ice Age triggered by volcanism and sustained by sea-ice/ocean feedbacks. Geophys. Res. Lett. 39, L02708. http://dx.doi.org/10.1029/2011GL050168.
Miller, G.H., Lehman, S.J., Refsnider, K.A., Southon, J.R., Zhong, Y., 2013. Unprecedented recent summer warmth in Arctic Canada. Geophys. Res. Lett. 40, 5745–5751. http://dx.doi.org/10.1002/2013GL057188.
Millet, L., Arnaud, F., Heiri, O., Magny, M., Verneaux, V., Desmet, M., 2009. Late-Holocene summer temperature reconstruction from chironomid assemblages of Lake Anterne, northern French Alps. Holocene 19 (2), 317–328.
Mom, V., Schultze, J., Wrobel, S., Eckstein, D., 2011. Which timbers were cleft from the same trees?. In: Proceedings of the 15th International Conference on Cultural Heritage and New Technologies, Vienna, Nov. 15-17, 2010. Vienna, pp. 582–591.
Mougin, P., 1912. Etudes Glaciologiques. In: Savoie – Pyrénées, Tome III. Imprimerie Nationale, Paris, 166 pp.
Müller, P., 1988. Parametrisierung der Gletscher-Klima-Beziehung für die Praxis, Grundlagen und Beispiele. Zürich, Mitteilungen der VAW/ETH-Zürich, 95, 228 pp.
Nesje, A., Lie, Ø., Dahl, S.O., 2000. Is the North Atlantic Oscillation reflected in Scandinavian glacier mass balance records? J. Quat. Sci. 15, 587–601.
Nicolussi, K., 2009. Klimaentwicklung in den Alpen während der letzten 7000 Jahre. In: Oeggl, K., Prast, M. (Eds.), Die Geschichte des Bergbaus in Tirol und seinen angrenzenden Gebieten. Impulsreferat zum 3. Milestone-Meeting des SFB HiMAT vom 23–26.10.2008 in Silbertal. Innsbruck University Press, pp. 109–124.
Nicolussi, K., Patzelt, G., 2001. Untersuchungen zur holozänen gletscherentwicklung von Pasterze und Gepatschferner (Ostalpen). Z. Gletscherkd. Glazialgeol. 36, 1–87.
Nicolussi, K., Schlüchter, C., 2012. The 8.2 ka event – calendar dated glacier response in the Alps. Geology 40, 819–822.
Nicolussi, K., Kaufmann, M., Patzelt, G., van der Plicht, J., Thurner, A., 2005. Holocene tree-line variability in the Kauner Valley, Central Eastern Alps, indicated by dendrochronological analysis of living trees and subfossil logs. Veg. Hist. Archaeobot. 14, 221–234.
Nicolussi, K., Jörin, U., Kaiser, K.F., Patzelt, G., Thurner, A., 2006. Precisely dated glacier fluctuations in the Alps over the last four millennia. In: Price, M.F. (Ed.), Global Change in Mountain Regions. Sapiens Publishing, pp. 59–60.
Nicolussi, K., Kauffmann, M., Melvin, T.M., Van Der Plicht, J., Schiessling, P., Thurner, A., 2009. A 9111 year long conifer tree ring chronology fort he European Alps: a base for environmental and climatic investigations. Holocene 19 (6), 909–920.
Nussbaumer, S.U., Zumbühl, H.J., 2012. The Little Ice Age history of the Glacier des Bossons (Mont Blanc area, France): a new high-resolution glacier length curve based on historical documents. Clim. Change 111 (2), 301–334.
Nussbaumer, S.U., Zumbühl, H.J., Steiner, D., 2007. Fluctuations of the Mer de Glace (Mont Blanc area, France) AD 1500-2050: an interdisciplinary approach using new historical data and neural network simulations. Z. Gletscherkd. Glazialgeol. 40, 1–183.
Nussbaumer, S.U., Steinhilber, F., Trachsel, M., Breitenmoser, P., Beer, J., Blass, A., Grosjean, M., Hafner, A., Holzhauser, H., Wanner, H., Zumbühl, H.J., 2011. Alpine climate during the Holocene: a comparison between records of glaciers, lake sediments and solar activity. J. Quat. Sci. 26 (7), 703–713.
Oerlemans, J., 2001. Glaciers and Climate Change. A.A. Balkema Publishers, 148 pp.
Olsen, J., Anderson, N.J., Knudsen, M.F., 2012. Variability of the North Atlantic Oscillation over the past 5,200 years. Nat. Geosci. 5, 808–812.

Orombelli, G., Porter, S., 1982. Late Holocene fluctuations of Brenva Glacier. Geogr. Fis. Din. Quaternario 5, 14–37.

Osborn, G., 1986. Lateral-moraine stratigraphy and Neoglacial history of Bugaboo Glacier, British Columbia. Quat. Res. 26, 171–178.

Osborn, G., Robinson, B.J., Luckman, B.H., 2001. Holocene and latest Pleistocene fluctuations of Stutfield Glacier, Canadian Rockies. Can. J. Earth Sci. 38, 1141–1155.

Osborn, G., Menounos, B., Ryane, C., Riedel, J., Clague, J.J., Koch, J., Clark, D., Scott, K., Davis, P.T., 2012. Latest Pleistocene and Holocene glacier fluctuations on Mount Baker, Washington. Quat. Sci. Rev. 49, 33–51.

Osborn, G., Haspel, R., Spooner, I., 2013. Late-Holocene fluctuations of the Bear River Glacier, northern Coast Ranges of British Columbia, Canada. Holocene 23 (3), 330–338.

PAGES 2k consortium, 2013. Continental-scale temperature variability during the past two millennia. Nat. Geosci. 6, 339–346.

Patzelt, G., 1995. Holocene glacier and climate variations - 7th Eastern Alps Traverse (D. van Husen). In: Schirmer, E. (Ed.), INQUA 1995 Quarternary Field Trips in Central Europe, vol. 1. Vlg. F. Pfeil, München, pp. 385–389.

Patzelt, G., Bortenschlager, S., 1973. Die postglazialen Gletscher- und Klimaschwankungen in der Venedigergruppe (Hohe Tauern, Ostalpen). Z. Geomorphol. N. F. Suppl. bd 16, 25–72.

Patzelt, G., Bortenschlager, S., Nicolussi, K., Poscher, G., 1990. Exkursionstagung Neue Ergebnisse der Holozänforschung in Tirol. Innsbruck, 45 pp.

Patzelt, G., Bortenschlager, S., Poscher, G., 1996. Exkursion A1 Tirol: Ötztal – Inntal. – DEUQUA 1996, Exkursionsführer, 23 pp.

Paul, F., Frey, H., Le Bris, R., 2011. A new glacier inventory for the European Alps from Landsat TM scenes of 2003: challenges and results. Ann. Glaciol. 52 (59), 144–152.

Pelfini, M., Belloni, S., Rossi, G., Strumia, G., 1997. Response time of Lys Glacier (Valle d'Aosta). An example of dendrogeomorphological and environmental study. Geogr. Fis. Din. Quat. 20, 329–338.

Pichler, T., Nicolussi, K., Goldenberg, G., Hanke, K., Kovács, K., Thurner, A., 2013. Charcoal from a prehistoric copper mine in the Austrian Alps: dendrochronological and dendrological data, demand for wood and forest utilisation. J. Archaeol. Sci. 40, 992–1002.

Rabatel, A., Letréguilly, A., Dedieu, J.-P., Eckert, N., 2013. Changes in glacier equilibrium-line altitude in the western Alps from 1984 to 2010: evaluation by remote sensing and modeling of the morpho-topographic and climate controls. Cryosphere 7, 1455–1471.

Ravanel, L., Allignol, F., Deline, P., Gruber, S., Ravello, M., 2010. Rockfalls in the Mont Blanc Massif in 2007 and 2008. Landslides 7, 493–501.

Reichert, B.K., Bengtsson, L., Oerlemans, J., 2001. Midlatitude forcing mechanisms for glacier mass balance investigated using general circulation models. J. Clim. 14, 3767–3784.

Reimer, P.J., Baillie, M.G.L., Bard, E., Bayliss, A., Beck, J.W., Blackwell, P.G., Bronk Ramsey, C., Buck, C.E., Burr, G.S., Edwards, R.L., Friedrich, M., Grootes, P.M., Guilderson, T.P., Hajdas, I., Heaton, T.J., Hogg, A.G., Hughen, K.A., Kaiser, K.F., Kromer, B., McCormac, F.G., Manning, S.W., Reimer, R.W., Richards, D.A., Southon, J.R., Talamo, S., Turney, C.S.M., van der Plicht, J., Weyhenmeyer, C.E., 2009. INTCAL 09 and MARINE09 radiocarbon age calibration curves, 0-50,000 years Cal BP. Radiocarbon 51 (4), 1111–1150.

Renner, F., 1982. Beiträge zur Gletschergeschichte des Gottardgebietes und dendroklimatologische Analysen an fossilen Hölzern. In: Physische Geographie, vol. 8. Zürich, 180 pp.

Reyes, A.V., Clague, J.J., 2004. Stratigraphic evidence for multiple Holocene advances of Lillooet Glacier, southern Coast mountains, British Columbia. Can. J. Earth Sci. 41, 903–918.

Reynaud, L., 1993. Glaciers of Europe-glaciers of the Alps: the French Alps. In: William Jr., R.S., Ferrigno, J.G. (Eds.), Satellite Image Atlas of Glaciers of the World, US Geol Surv Prof Pap 1386E, pp. E23–E36.

Reynaud, L., Vincent, C., 2000. Relevés de fluctuations sur quelques glaciers français. La Houille Blanche 5, 79–86.

RinnTech, 2005. TSAP-Win. Time Series Analysis and Presentation for Dendrochronology and Related Application. Version 0.53. www.rinntech.com.

Robock, A., 2000. Volcanic eruptions and climate. Rev. Geophys. 38 (2), 191–219.

Röthlisberger, F., 1976. Gletscher- und Klimaschwankungen im Raum Zermatt, Ferpecle und Arolla. Die Alp. 52, 59–152.

Röthlisberger, F., Schneebeli, W., 1979. Genesis of lateral moraine complexes, demonstrated by fossil soils and trunks: indicators of postglacial climatic fluctuations. In: Schlüchter, C. (Ed.), Moraines and Varves. Balkema, Rotterdam, pp. 387–419.

Röthlisberger, H., Haas, P., Holzhauser, H., Keller, W., Bircher, W., Renner, F., 1980. Holocene climatic fluctuations - radiocarbon dating of fossil soils (fAh) and woods from moraines and glaciers in the Alps. Geogr. Helv. 35 (5), 21–52.

Reyes, A.V., Wiles, G.C., Smith, D.J., Barclay, D.J., Allen, S., Jackson, S., Larocque, S., Laxton, S., Lewis, D., Calkin, P.E., Clague, J.J., 2006. Expansion of alpine glaciers in Pacific North America in the first millennium A.D. Geology 34, 57–60.

Ryder, J.M., Thomson, B., 1986. Neoglaciation in the southern Coast Mountains, British Columbia: chronology prior to the Neoglacial maximum. Can. J. Earth Sci. 24, 1294–1301.

Salzer, M.W., Hughes, M.K., 2007. Bristlecone Pine tree rings and volcanic eruptions over the last 5000 years. Quat. Res. 67, 57–68.

Schimmelpfennig, I., Schaefer, J.M., Akçar, N., Ivy-Ochs, S., Finkel, R.C., Schlüchter, C., 2012. Holocene glacier culminations in the Western Alps and their hemispheric relevance. Geology 40, 891–894.

Schimmelpfennig, I., Schaefer, J.M., Akçar, N., Koffman, T., Ivy-Ochs, S., Schwartz, R., Finkel, R.C., Zimmerman, S., Schlüchter, C., 2014. A chronology of Holocene and Little Ice Age glacier culminations of the Steingletscher, Central Alps, Switzerland, based on high-sensitivity beryllium-10 moraine dating. Earth Planet. Sci. Lett. 393, 220–230.

Schmeits, M.J., Oerlemans, J., 1997. Simulation of the historical variations in length of the Unterer Grindelwaldgletscher. J. Glaciol. 43, 152–164.

Schmidt, R., Roth, M., Tessadri, R., Weckström, K., 2008. Disentangling late-Holocene climate and land use impacts on an Austrian alpine lake using seasonal temperature anomalies, ice-cover, sedimentology, and pollen tracers. J. Paleolimnol. 40, 453–469.

Schneebeli, W., 1976. Untersuchungen von Gletscherschwankungen im Val de Bagnes. Die Alp. 52, 5–57.

Schurer, A.P., Tett, S.F.B., Hegerl, G.C., 2014. Small influence of solar variability on climate over the past millennium. Nat. Geosci. 7, 104–108.

Schweingruber, F.H., 1990. Microscopic Wood Anatomy; Structural Variability of Stems and Twigs in Recent and Subfossil Woods from Central Europe, third ed. Eidgenössische Forschungsanstalt WSL, Birmensdorf.

Schweingruber, F.H., 2007. Wood structure and Environment. In: Springer Series in Wood Science. Springer, Heidelberg, 279 pp.

Shapiro, A.I., Schmutz, W., Rozanov, E., Schoell, M., Haberreiter, M., Shapiro, A.V., Nyeki, S., 2011. A new approach to long-term reconstruction of the solar irradiance leads to large historical solar forcing. Astron. Astrophys. 529, A67.

Sigl, M., McConnell, J.R., Layman, L., Maselli, O., McGwire, K., Pasteris, D., Dahl-Jensen, D., Steffensen, J.P., Vinther, B., Edwards, R., Mulvaney, R., Kipfstuhl, S., 2013. A new bipolar ice core record of volcanism from WAIS Divide and NEEM and implications for climate forcing of the last 2000 years. J. Geophys. Res. Atmos. 118, 1151–1169. http://dx.doi.org/10.1029/2012JD018603.

Simonneau, A., Chapron, E., Garçon, M., Winiarski, T., Graz, Y., Chauvel, C., Debret, M., Motelica-Heino, M., Desmet, M., Di Giovanni, C., 2014. Tracking Holocene glacial and high-altitude alpine environments fluctuations from minerogenic and organic markers in proglacial lake sediments (Lake Blanc Huez, Western French Alps). Quat. Sci. Rev. 89, 27–43.

Six, D., Vincent, C., 2014. Sensitivity of mass balance and equilibrium-line altitude to climate change in the French Alps. J. Glaciol. 60 (223), 867–878.

Six, D., Reynaud, L., Letréguilly, A., 2001. Bilans de masse des glaciers alpins et scandinaves, leurs relations avec l'oscillation du climat de l'Atlantique nord. C. R. Acad. Sci. Paris 333, 693–698.

Steinhilber, F., Beer, J., Fröhlich, C., 2009. Total solar irradiance during the Holocene. Geophys. Res. Lett. 36, L19704.

Steinhilber, F., Abreu, J.A., Jürg Beer, J., Brunner, I., Christl, M., Fischer, H., Heikkilä, U., Kubik, P.W., Mann, M., McCracken, K.G., Miller, H., Miyahara, H., Oerter, H., Wilhelms, F., 2012. 9,400 years of cosmic radiation and solar activity from ice cores and tree rings. PNAS 109 (16), 5967–5971.

Stenchikov, G., Delworth, T.L., Ramaswamy, V., Stouffer, R.J., Wittenberg, A., Zeng, F., 2009. Volcanic signals in oceans. J. Geophys. Res. 114, D16104. http://dx.doi.org/10.1029/2008JD011673.

Stuiver, M., Reimer, P.J., Reimer, R., 2011. CALIB Radiocarbon Calibration Version 6.0.1 [WWW program and documentation]. http://radiocarbon.pa.qub.ac.uk/calib/.

Tegel, W., Elburg, R., Hakelberg, D., Stäuble, H., Büntgen, U., 2012. Early Neolithic water wells reveal the world's oldest wood architecture. PLoS One 7 (12), e51374.

Telford, R.J., Heegaard, E., Birks, H.J.B., 2004. The intercept is a poor estimate of a calibrated radiocarbon age. Holocene 14, 296–298.

Tinner, W., Theurillat, J.P., 2003. Uppermost limit, extent, and fluctuations of the timberline and treeline ecocline in the Swiss Central Alps during the past 11 500 years. Arct. Antarct. Alp. Res. 35 (2), 158–169.

Thibert, E., Eckert, N., Vincent, C., 2013. Climatic drivers of seasonal glacier mass balances: an analysis of 6 decades at Glacier de Sarennes (French Alps). Cryosphere 7, 47–66.

Trachsel, M., Kamenik, C., Grosjean, M., McCarroll, D., Moberg, A., Brázdil, R., Büntgen, U., Dobrovolný, P., Esper, J., Frank, D.C., Friedrich, M., Glaser, R., Larocque-Tobler, I., Nicolussi, K., Riemann, D., 2012. Multi-archive summer temperature reconstruction for the European Alps, AD 1053–1996. Quat. Sci. Rev. 46, 66–79.

Tyndall, J., 1873. Les glaciers et les transformations de l'eau. Germer Baillière, Paris, 268 pp.

van Geel, B., Mauquoy, D., 2010. Peatland records of solar activity: rainwater-fed Holocene raised bog deposits in temperate climate zones are valuable archives of solar activity fluctuations and related climate changes. PAGES News 18, 11–14.

Vallot, J., 1900. Annales de l'observatoire météorologique, physique et glaciaire du Mont Blanc. Tome 4. Steinheil, Paris, 189 pp.

Vincent, C., 2010. L'impact des changements climatiques sur les glaciers alpins (PhD thesis). Joseph Fourier University, 211 pp.

Vincent, C., Harter, M., Gilbert, A., Berthier, E., Six, D., 2014. Future fluctuations of Mer de Glace, French Alps, assessed using a parameterized model calibrated with past thickness changes. Ann. Glaciol. 55 (66), 15–24.

Viollet-le-Duc, E., 1876. Le massif du Mont Blanc. Etude sur sa constitution géodésique et géologique, sur ses transformations et sur l'état ancien et moderne de ses glaciers. Baudry, Paris, 280 pp.

Vivian, R., 1975. Les glaciers des Alpes Occidentales. Allier, Grenoble, 516 pp.

Vollweiler, N., Scholz, D., Mühlinghaus, C., Mangini, A., Spötl, C., 2006. A precisely dated climate record for the last 9 kyr from three high alpine stalagmites, Spannagel Cave, Austria. Geophys. Res. Lett. 33 (L20703), 324. http://dx.doi.org/10.1029/2006GL027662.

Wanner, H., Broennimann, S., Casty, C., Gyalistras, D., Luterbacher, J., Schmutz, C., Stephenson, D.B., Xoplaki, E., 2001. North Atlantic Oscillation – concepts and studies. Surv. Geophys. 22, 321–382.

Wanner, H., Beer, J., Bütikofer, J., Crowley, T.J., Cubasch, U., Flückiger, J., Goosse, H., Grosjean, M., Joos, F., Kaplan, J.O., Küttel, M., Müller, S.A., Prentice, I.C., Solomina, O., Stocker, T.F., Tarasov, P., Wagner, M., Widmann, M., 2008. Mid- to Late Holocene climate change: an overview. Quat. Sci. Rev. 27, 1791–1828.

Wanner, H., Solomina, O., Grosjean, M., Ritz, S.P., Jetel, M., 2011. Structure and origin of Holocene cold events. Quat. Sci. Rev. 30, 3109–3123.

Wegmann, M., Brönnimann, S., Bhend, J., Franke, J., Folini, D., Luterbacher, M.W.J., 2014. Volcanic influence on European summer precipitation through monsoons: possible cause for "Years without Summer". J. Clim. http://dx.doi.org/10.1175/JCLI-D-13-00524.1.

Wetter, W., 1987. Spät- und Post-glaziale Gletscherschwankungen im Mont Blanc Gebiet: Untere Vallée de Chamonix-Val Montjoie. In: Physische Geographie, vol. 22. Zürich, 269 pp.

Wiles, G.C., D'Arrigo, R.D., Villalba, R., Calkin, P.E., Barclay, D.J., 2004. Century-scale solar variability and Alaskan temperature change over the past millennium. Geophys. Res. Lett. 31, L15203. http://dx.doi.org/10.1029/200GL020050.

Wiles, G.C., Lawson, D.E., Lyon, E., Wiesenberg, N., D'Arrigo, R.D., 2011. Tree-ring dates on two pre-Little Ice Age advances in Glacier Bay National Park and Preserve, Alaska, USA. Quat. Res. 76, 190–195.

Winkler, S., Hagedorn, H., 1999. Lateralmoränen – Morphologie, Genese und Beziehung zu Gletscherstandsschwankungen (Beispiele aus Ostalpen und West-/Zentralnorwegen). Z. Geomorphol. N.F. Suppl. Bd 113, 69–84.

Winkler, S., Matthews, J.A., 2010. Holocene glacier chronologies: are 'high-resolution' global and inter-hemispheric comparisons possible? Holocene 20 (7), 1137–1147.

Wipf, A., 2001. Gletschergeschichtliche Untersuchungen im Spät- und Postglazialen Bereich des Hinteren Lauterbrunnentals (Berner Oberland, Schweiz). Geogr. Helv. 56 (2), 133–144.

Zanesco, A., Nicolussi, K., Patzelt, G., 2008. Die Überschwemmung der Unterstadt von Hall im Jahr 1275. In: Zanesco, A., Schmitz-Esser, R. (Eds.), Neues zur Geschichte der Stadt. Forum Hall in Tirol 2, pp. 40–53.

Zoller, H., Schindler, C., Röthlisberger, H., 1966. Postglaziale Gletscherstände und Klimaschwankungen im Gotthardmassiv und Vorderrheingebiet. Verh. Naturforsch. Ges. Basel 77, 97–164.

Zumbühl, H.J., 1980. Die Schwankungen der Grindelwaldgletscher in den historischen Bild- und Schriftquellen des 12. bis 19. Jahrhunderts. Ein Beitrag zur Gletschergeschichte und Erforschung des Alpenraumes. In: Denkschriften der Schweizerischen Naturforschenden Gesellschaft (SNG), Band 92. Birkhäuser, Basel/Boston/Stuttgart, 279 pp.

Zumbühl, H.J., Holzhauser, H., 1988. Alpengletscher in der Kleinen Eiszeit. Die Alpen 64 (3), 129–322.

Zuo, Z., Oerlemans, J., 1997. Numerical modelling of the historic front variation and the future behaviour of the Pasterze glacier, Austria. Ann. Glaciol. 24, 234–241.